Trauma

17

Vikas Jain, and Toshio Moritani

Hiroto Kawasaki

17.1 Introduction

Traumatic brain injuries (TBI) are a common cause of significant morbidity and mortality worldwide. They are the most common cause of death and permanent disability in the early decades of life. Approximately 1.7 million people are affected by TBI in the USA every year, out of which 275,000 patients are admitted. TBI leads to approximately 52,000 deaths annually in the USA [1, 2]. The victims vary widely with regard to their etiology, clinical presentation, pathophysiology, and optimal treatment strategies.

Traumatic brain injuries may be focal or diffuse or a combination of both. Focal brain injuries are usually due to direct impact and result in contusions and extra axial hematomas. Diffuse brain injuries are usually caused by acceleration/deceleration injuries and are typically seen following high velocity vehicular accidents or shaken baby syndrome. The clinical sequelae can include concussions and/or diffuse axonal injury. Traumatic axonal injury (TAI) results from shear injuries that reflect sudden acceleration and deceleration as well as rotational strain which result in hemorrhagic and nonhemorrhagic foci at gray-white matter junctions, in the corpus callosum and in the dorsolateral aspect of the brainstem. The term diffuse axonal injury (DAI) is defined by three or more lesions in two or more lobes and corpus callosum [2].

Many of the survivors may suffer significant long-term consequences. DAI is a major pathologic substrate of unconsciousness, persistent vegetative state, neurological deficits, and cognitive decline.

Diagnostic neuroimaging plays a pivotal role in the management of these injuries. Non-contrast CT scan of the head is the initial modality of choice by consensus and provides extremely valuable information for triage and trauma patient management. Head CT is excellent for showing traumatic lesions which require immediate surgical intervention such as decompressive craniotomy or craniectomy, hematoma evacuation, and ventriculostomy catheter placement. However, CT is very insensitive in the detection of TAI/DAI and grossly underestimates nonhemorrhagic contusions especially in the acute setting. MRI, particularly diffusion-weighted image (DWI), fluid attenuated inversion recovery (FLAIR),

V. Jain (✉)
Department of Radiology, MetroHealth Medical Center, Case Western Reserve University, Cleveland, OH, USA

T. Moritani
Department of Radiology, Division of Neuroradiology, Clinical Neuroradiology Research, University of Michigan, Ann Arbor, MI, USA
e-mail: tmoritan@med.umich.edu

H. Kawasaki
University of Iowa Hospitals & Clinics, Iowa City, IA, USA
e-mail: hiroto-kawasaki@uiowa.edu

T2*-weighted gradient-echo (GRE), and susceptibility-weighted image (SWI) sequences, is much more sensitive than CT scan for the detection of such TAI/DAI. MR is however performed in relatively few selected patients, generally where there is mismatch between the CT findings and neurological symptoms or clinical examination [3–5].

17.2   Diffuse Axonal Injury

Strich and colleagues first described DAI in 1956 and it was later characterized by Adams and coworkers, who linked the histopathological features of post-traumatic damage in the axons to rotational acceleration-deceleration forces to the head that result in stretch injuries [6, 7].

DAI refers to the shear injury at the tissue interfaces with different density and is classically located at gray white matter junctions such as the centrum semiovale, corpus callosum, internal capsules, fornix, posterolateral aspect of the upper brainstem, and cerebellar peduncles. DAI may be confined to the white matter of the frontal and temporal lobes in mild head trauma (Fig. 17.1). Lesions in the posterior half of the corpus callosum indicate more severe injury. With even more severe injuries, DAI lesions may be seen in the anterior corpus callosum and dorsolateral aspect of the upper brainstem (Figs. 17.2 and 17.3). DAI lesions may also be seen, but less commonly, in other areas of the brain such as the parietal and occipital lobes, internal and external capsules, basal ganglia, thalami, fornix, and septum pellucidum (Fig. 17.4). Intraventricular hemorrhage may be seen in some patients due to disruption of the subependymal plexus of capillaries and veins lining the ventricular surface of the corpus callosum, septum pellucidum, and fornix [4, 8, 9].

DAI lesions are usually multiple, diffuse, small (5–15 mm), and mainly T2-hyperintense foci which are generally limited to white matter and are rarely seen on standard CT scans. 10–30% of the DAI lesions are hemorrhagic [4, 8] (Fig. 17.3).

DAI is a common finding in patients suffering from severe TBI and is a more important predictor of poor neurological outcome and long-term outcome with respect to cognition and behavior impairment than focal TBI [10]. The consequences are often devastating, and the presence of DAI is a major adverse prognostic factor in the majority of affected patients. These patients also usually develop global atrophy after few months.

Clinically, DAI typically manifests as impaired consciousness and coma shortly after trauma due to acute injury to the axons. While the axons are injured on initial impact due to shearing injury, major damage to the axons continues to propagate after the traumatic event because of delayed activation of complex biochemical processes in the cells [11].

Pathologically, injury related to DAI is always much more extensive microscopically than at gross examination or as seen on imaging. Microscopically, shearing injuries initially produce multiple, characteristic axonal bulbs, or retraction balls, as well as numerous foci of perivascular hemorrhage [1, 12, 13].

17.3   Grading of DAI and Location

There are three grades of DAI in the Adams classification which was first proposed by J.H. Adams and associates in 1989; these grades are based on the anatomic distribution of the injury and have been shown to have a direct relationship to the severity of injury and adverse outcomes [6].

Grade I is presence of lesions at gray white matter junctions, which are most commonly seen in the parasagittal regions of the frontal lobes and periventricular temporal lobes. Parietal and occipital lobes, cerebellum, and internal capsules are less commonly involved. DAI may be confined to the white matter of the frontal and temporal lobes in mild head trauma [9] (Fig. 17.5).

Grade II includes involvement of the corpus callosum in addition to grade I lesions and is seen in approximately 20% of patients. The posterior body and splenium of the corpus callosum are most commonly affected with progression anteriorly as the severity increases (Fig. 17.6).

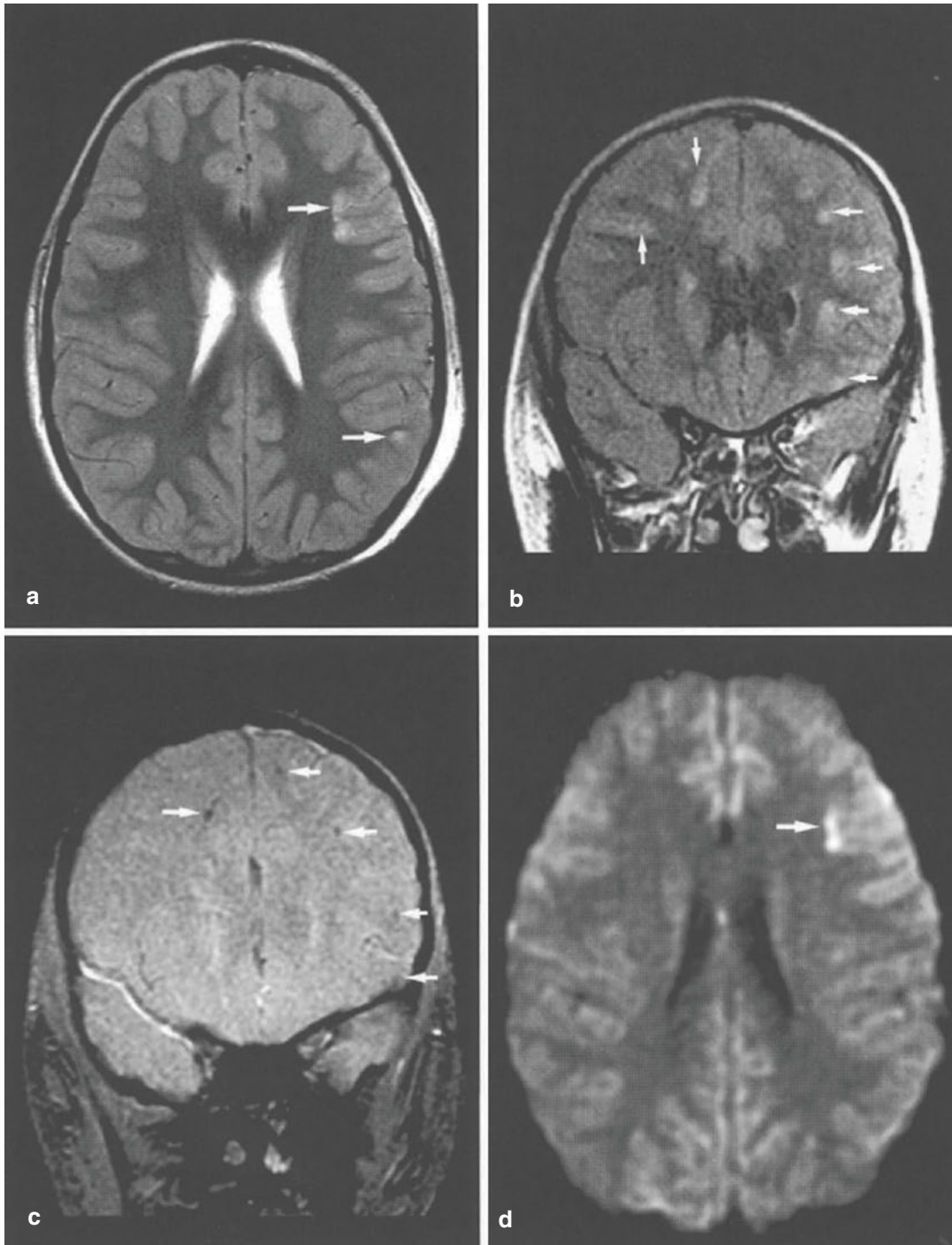Grade III is defined by lesions in the dorsolateral brainstem (Fig. 17.7).

Fig. 17.1 (**a–d**) Diffuse axonal injury in gray-white matter junction in a 7-year-old boy after a motor vehicle accident. (**a**, **b**) T2-weighted and coronal FLAIR images show multiple hyperintense lesions in the gray-white matter junction of bilateral frontoparietal lobes (*arrows*). (**c**) Coronal GRE image shows multiple small hemorrhages as low signal in these lesions (*arrows*). (**d**) DW image demonstrates diffuse axonal injury as high signal intensity (*arrow*) with decreased ADC (not shown), representing cytotoxic edema
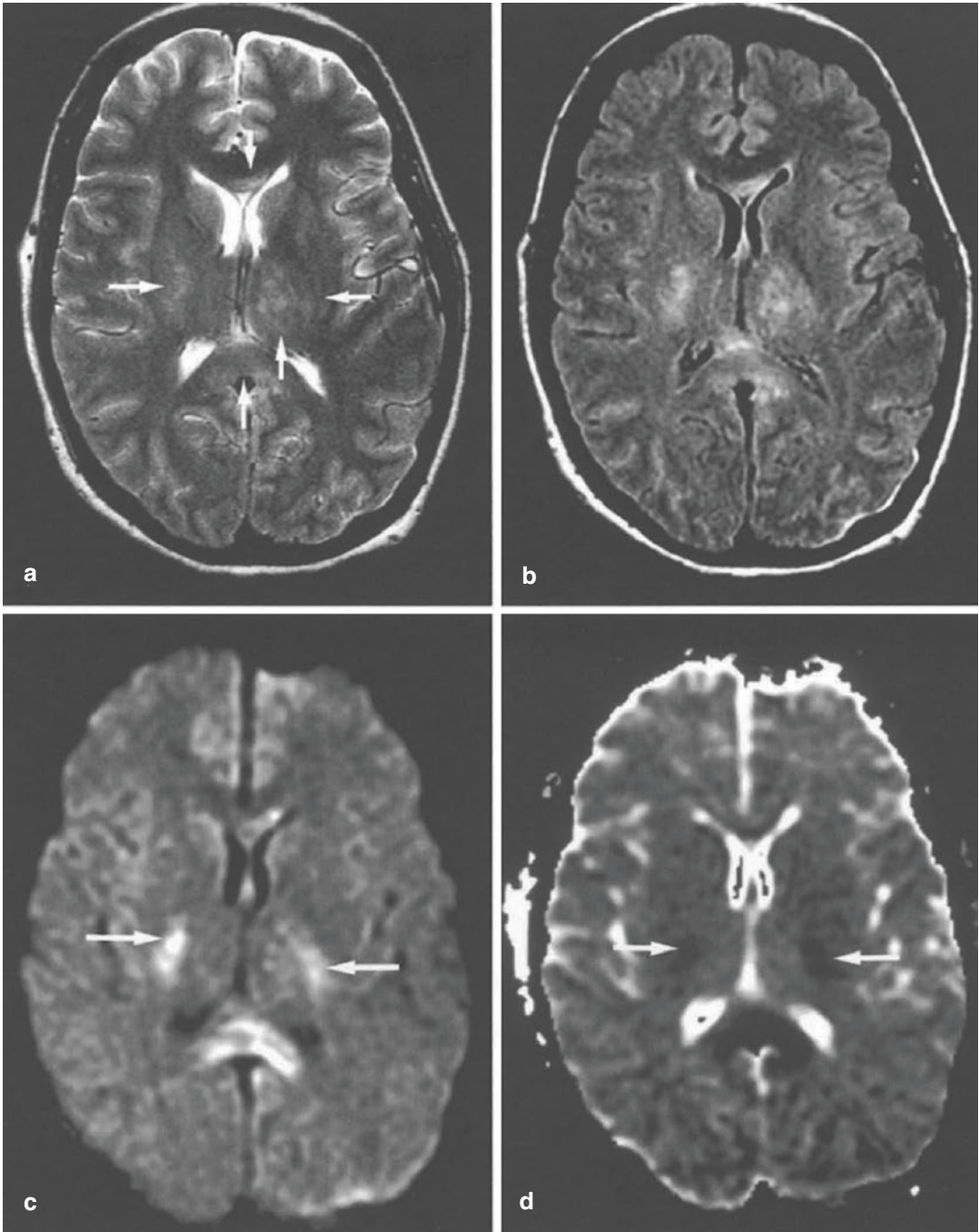
Fig. 17.2 (**a**–**d**) Diffuse axonal injury in the corpus callosum, internal capsule, and thalamus in a 29-year-old woman after a motor vehicle accident. (**a**, **b**) T2-weighted and FLAIR images show multiple hyperintense lesions in the anterior and posterior corpus callosum, internal capsules, and left thalamus (*arrows*). (**c**, **d**) DW image demonstrates these lesions as high signal intensity with decreased ADC (*arrows*)
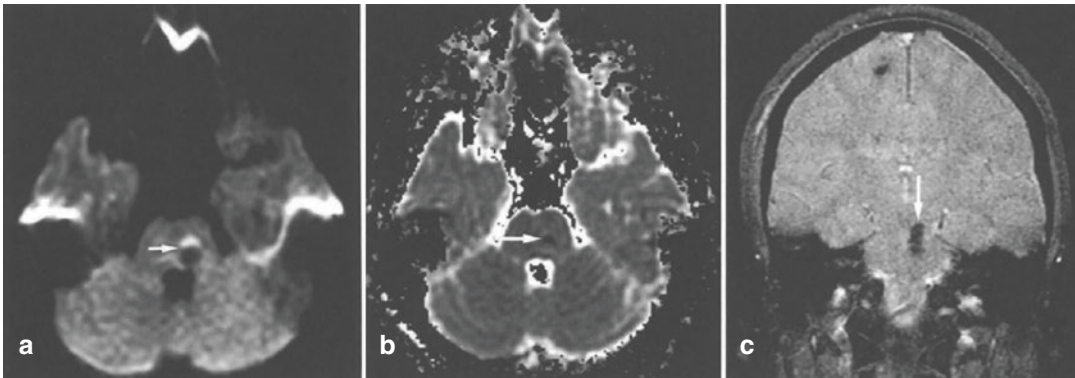
Fig. 17.3 (**a**–**c**) Diffuse axonal injury in the brain stem in a 28-year-old man after a motor vehicle accident. (**a**) DW image shows a hypointense lesion with a hyperintense rim in the dorsolateral aspect of the midbrain, representing a hemorrhagic lesion of diffuse axonal injury (*arrow*). (**b**) ADC map shows decreased ADC of this lesion (*arrow*). This might be due to a paramagnetic susceptibility artifact. (**c**) Coronal GRE image clearly shows hemorrhagic lesions as hypointense in the brain stem (*arrow*) and in the right frontoparietal region

Intraventricular hemorrhage can accompany these findings. They have the same mechanical origin and are due to disruption of the subependymal plexus of capillaries and veins that lie along the ventricular surface of the corpus callosum, fornix, and septum pellucidum [8, 9, 14, 15] (Figs. 17.8 and 17.14).

Hamdeh et al. conducted a study on 30 patients with severe DAI (Glasgow Motor Scale of <6) examined with MRI within one-week post injury and concluded after multivariate analysis that there was an independent indicator of poor outcome for patients with lesions in the substantia nigra and tegmentum on SWI. They found that lesions seen in these areas have a worse outcome than patients with lesions in other parts of the brainstem [10].

Once it was thought that edema following traumatic brain injury was vasogenic, but recent experimental studies using diffusion-weighted imaging (DWI) have shown that edema after head trauma consists of both vasogenic and cytotoxic edema [3, 16–19]. Since DW imaging is also very sensitive in detecting small lesions of cytotoxic edema and can differentiate cytotoxic from vasogenic edema, it has become especially useful in the evaluation and staging of patients with DAI.

17.4 Computed Tomography (CT) and Magnetic Resonance (MR) Imaging

Few DAI lesions are visible on head CT. Only large lesions or those that are grossly hemorrhagic are seen. MR imaging has been proven to be more sensitive for detection as well as for characterization of DAI lesions. Conventional MR imaging shows multiple, small, deeply situated elliptical lesions that spare the overlying cortex. MRI is also more sensitive to detect subtle and early ischemic changes and contusions on the surface of the brain (Figs. 17.7 and 17.9). FLAIR images are more sensitive than T2-weighted images to detect small hyperintense lesions adjacent to the cerebrospinal fluid, such as in the fornix and septum pellucidum [4, 14, 20, 21]. DWI has been found to be equally or more sensitive than FLAIR in multiple studies.

Nonhemorrhagic lesions (NHL) are more numerous than hemorrhagic lesions. While DWI can also detect some hemorrhagic lesions, GRE and SWI are more sensitive for detecting hemorrhagic lesions. Small hemorrhagic lesions are seen in 10–30% of all DAI lesions and are best detected on GRE images because of their susceptibility effects. SWI uses the magnetic sus-
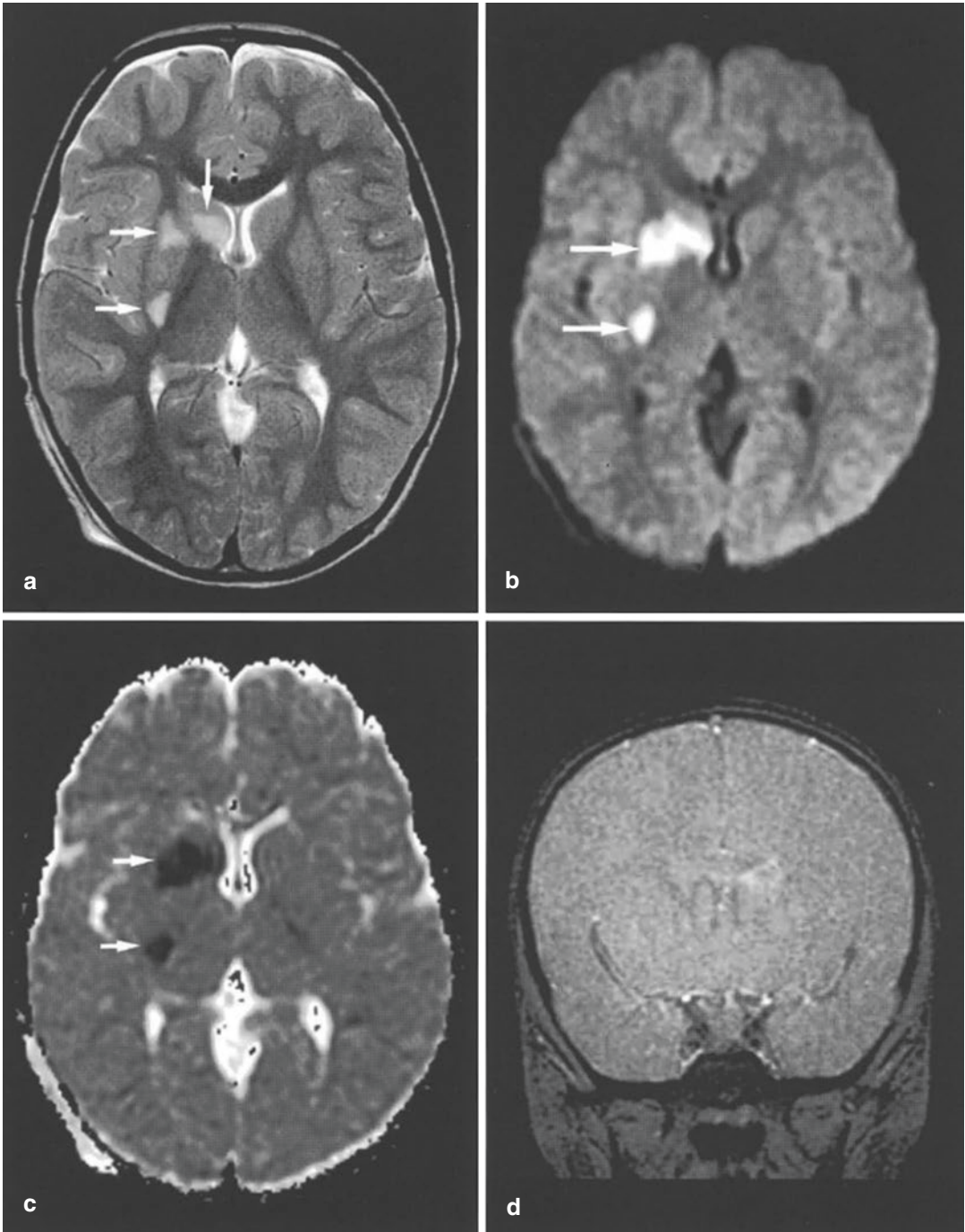
Fig. 17.4 (**a–d**) Diffuse axonal injury in the basal ganglia in a 3-year-old boy after a motor vehicle accident. (**a**) T2-weighted image shows hyperintense lesions in the right lentiform and caudate nucleus (*arrows*). (**b**, **c**) DW imaging shows these lesions as hyperintense with decreased ADC (*arrows*). (**d**) Coronal GRE image clearly shows no hemorrhagic foci in these lesions
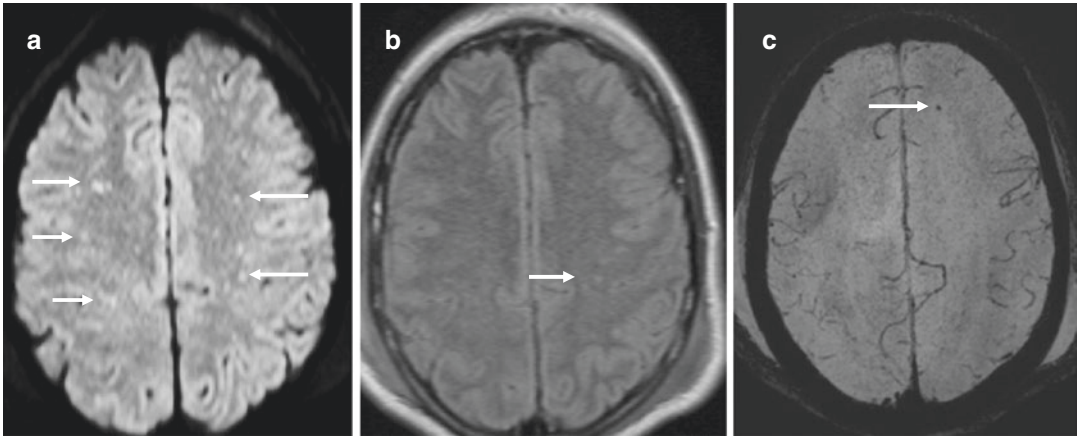
Fig. 17.5 (**a–c**) DAI grade 1 in a 34-year-old male after MVA. CT head was negative (not shown). (**a**) DWI shows multiple tiny foci of RD (decreased ADC not shown) in bilateral cerebral hemispheres. (**b**) FLAIR shows fewer lesions which are very subtle. (**c**) SWI shows only one lesion in the left frontal lobe which was also seen on the DWI. Adam's grade I DAI as lesions are seen only in the cerebral hemispheres, without involvement of the corpus callosum or brainstem
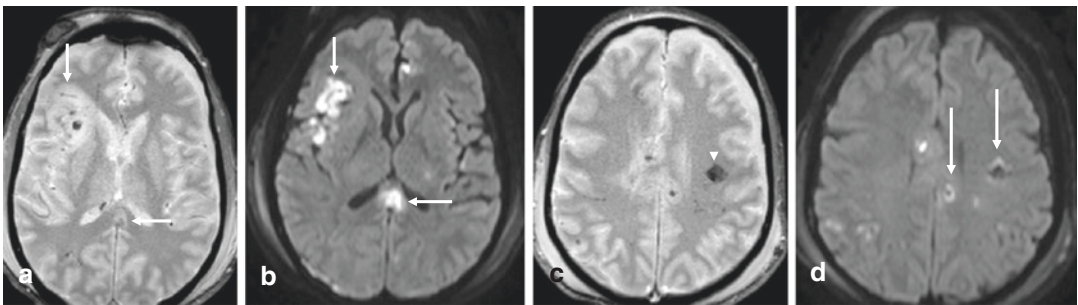

Fig. 17.6 (**a–d**) DAI grade 2. 25-year-old female after high-speed MVA. Multiple nonhemorrhagic and hemorrhagic (arrowhead in **c**) lesions seen on DWI (**b**, **d**) and GRE (**a**, **c**) sequences. The nonhemorrhagic DAI lesions in the splenium of the corpus callosum (**b**) and near the right sylvian fissure (**b**) are better seen on DWI. DWI is more sensitive for nonhemorrhagic lesions. DWI can also detect hemorrhagic DAI lesions but is less sensitive than GRE. Hemorrhagic DAI lesions appear as central areas of hypointensity surrounded by peripheral halo of hyperintensity on DWI images (long arrows in **d**)
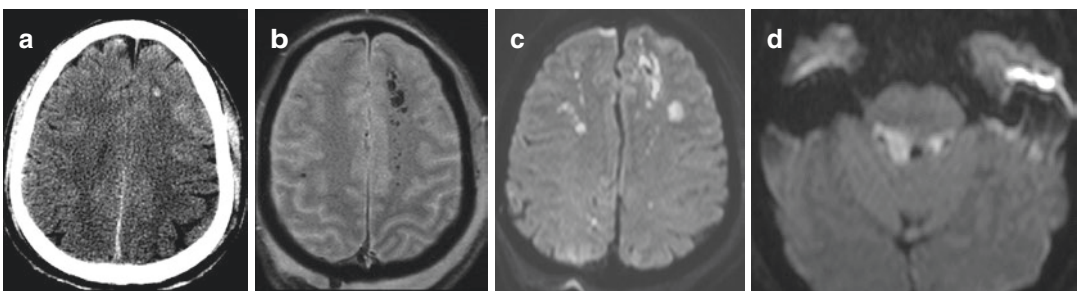

Fig. 17.7 (**a–d**) DAI grade III. 25-year-old male with altered metal status after high-speed MCC. A mixture of hemorrhagic and nonhemorrhagic DAI in bilateral frontal lobes. CT (**a**) shows only one hemorrhagic lesion. Many nonhemorrhagic lesions seen on DWI (**c**) are not seen on GRE (**b**). Multiple DAI lesions seen in the cerebral hemispheres and in the posterior aspect of the brainstem on both sides (**c** and **d**). DAI lesions in the brainstem (**d**) indicates Adam's Grade III DAI and are associated with a poorer prognosis

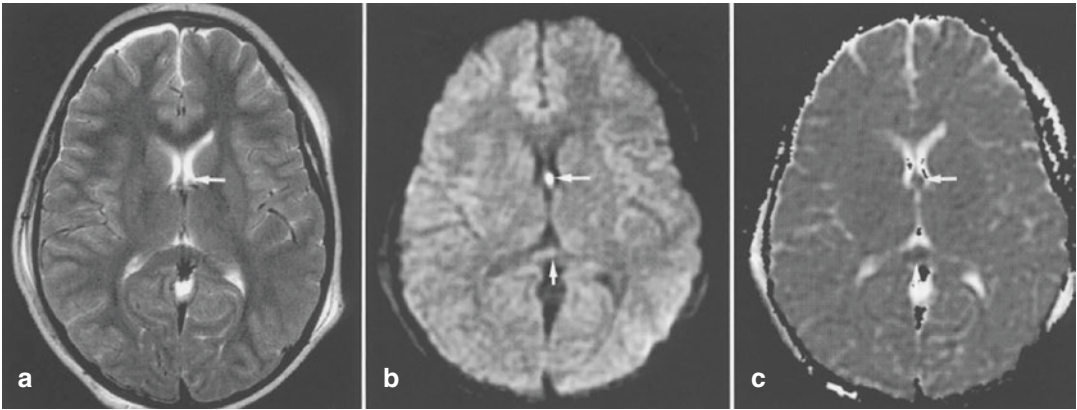**Fig. 17.8** (**a**–**c**) Diffuse axonal injury in the fornix of an 11-year-old girl after a motor vehicle accident. (**a**) On T2-weighted image, it is difficult to detect a small hyper-intense lesion in the fornix (*arrow*). (**b**, **c**) DW image shows the lesion in the fornix and posterior corpus callosum as hyperintense with decreased ADC (*arrows*)
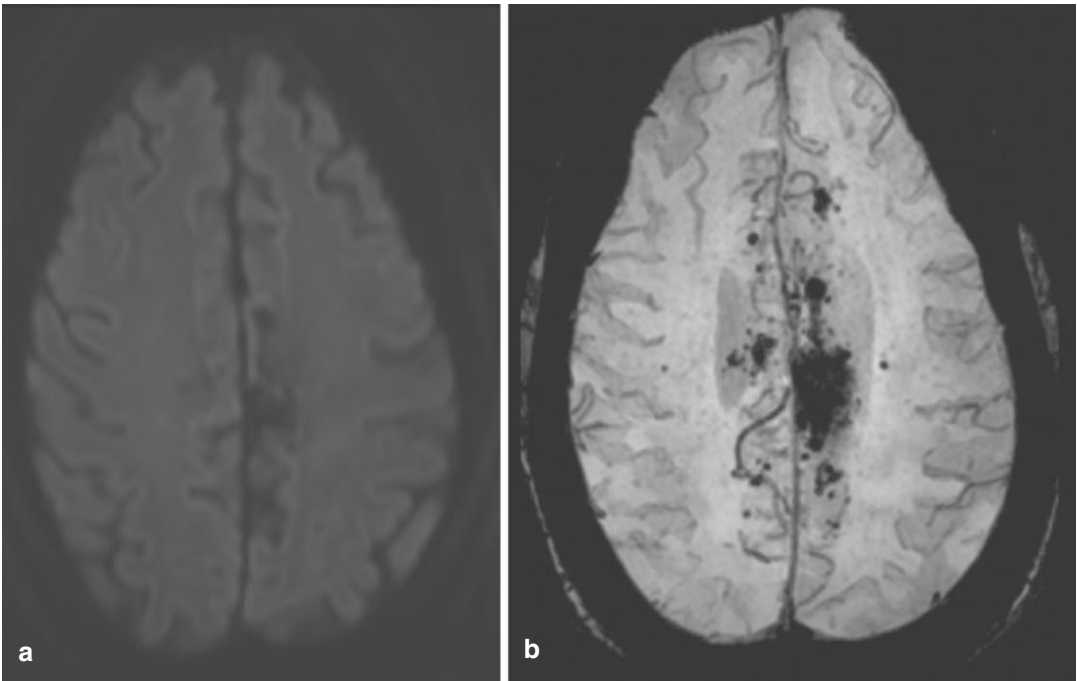

Fig. 17.9 (**a**–**d**) 32-year-old male with high-speed MVA presenting with altered mental status. Acute to subacute SDH can appear hyperintense on DWI (**a**) and hypointense on ADC maps (**b**). The T1 image (**c**) shows curvilinear hyperintensity and CT scan (**d**) shows curvilinear hyperdensity because of SDH over the left convexity. The underlying brain parenchyma adjacent to the SDH also shows RD (arrows in **a** and **b**) suggestive of ischemic injury secondary to SDH and trauma

ceptibility differences between various tissues, which gives phase differences between the regions which contain paramagnetic deoxygenated blood products and normal surrounding tis-sues. SWI is 3–6 times more sensitive than GRE in detecting the size, number, volume, and distribution of hemorrhagic foci of DAI. However, even these MR imaging sequences are thought
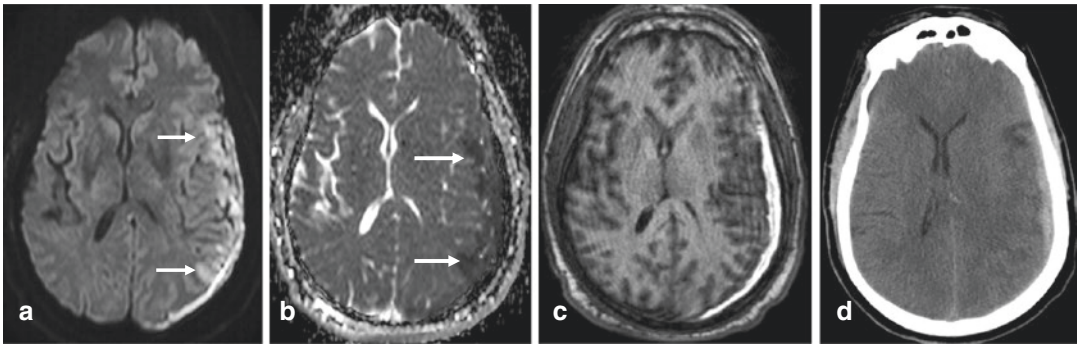
Fig. 17.10 (**a**–**b**) MRI of a 55-year-old male after MVA shows multiple hemorrhagic foci in bilateral cerebral hemispheres seen on SWI (**b**) which were not as conspic- uous on DWI (**a**). SWI or GRE are more sensitive for detecting hemorrhagic lesions

to underestimate the true extent of DAI [20–23] (Fig. 17.10).

Traumatic midline SAH in the perimesence- phalic cistern and interhemispheric fissure on the initial CT scan after trauma has been found to strongly implicate shearing injury and severe DAI in a study conducted by Meta-Mbemba et al. They reported sensitivity of 60.8% and specific- ity of 81.7% for severe DAI in a study on 270 patients with history of head trauma [24].

## 17.5 Diffusion-Weighted Imaging (DWI)

DWI measures a unique physiological parameter characterized by random microscopic motion of water molecules in the tissues which can define types of edema in various conditions. DWI can detect lesions with both increased/ facilitated dif- fusion and restricted diffusion (RD). Lesions with increased/ facilitated diffusion are bright on both DWI and ADC maps and have increased extracellular water where water molecules are more mobile. This finding reflects vasogenic edema which is usually reversible. These lesions appear hyperintense on DWI due to T2 shine through. The diffusion maps are generated with combined input from diffusion-weighted and T2-weighted properties and therefore lesions with long T2 relaxation time will also be bright on DWI. This effect is removed on ADC maps,

which represent the apparent diffusion coeffi- cient [25–28].

The lesions with cytotoxic edema show restricted diffusion and are bright on DWI and dark on ADC maps; this is the classic pattern of acute infarcts. This phenomenon results from the shift of freely mobile water molecules from the extracellular space to the intracellular space where movement of water molecules is restricted. This indicates cellular swelling and cytotoxic edema, which usually are considered irreversible injury and cell death, with few exceptions.

The exact mechanism of RD in DAI is still uncertain, and proposed mechanisms include excitotoxic edema due to release of a high con- centration of glutamate and other neurotransmit- ters, associated hypotension and hypoxia leading to trauma induced ischemia or collapse of the cytoskeleton of injured axons [15, 27, 29, 30] (Fig. 17.11). There is increase in extracellular levels of amino acids glutamate and aspartate after TBI, and experiments have shown that N-methyl-D aspartate (NMDA) receptor antagonists have protective role. Glutamate receptor antagonists help the neurons to deal with the increased permeability of the cell membrane to ions as well as reduced efficacy of Na + extru- sion [31, 32]. Damage at the node of Ranvier results in a traumatic defect in the axonal mem- brane. This defect causes excessive neurotrans- mitter release with increase in intracellular

Fig. 17.11 Leakage of glutamate in diffuse axonal injury. Diffuse axonal injury is presumably due to the leakage of glutamate at the node of Ranvier. The astrocytic end-foot is located on the axon at the node of Ranvier and may protect the axons
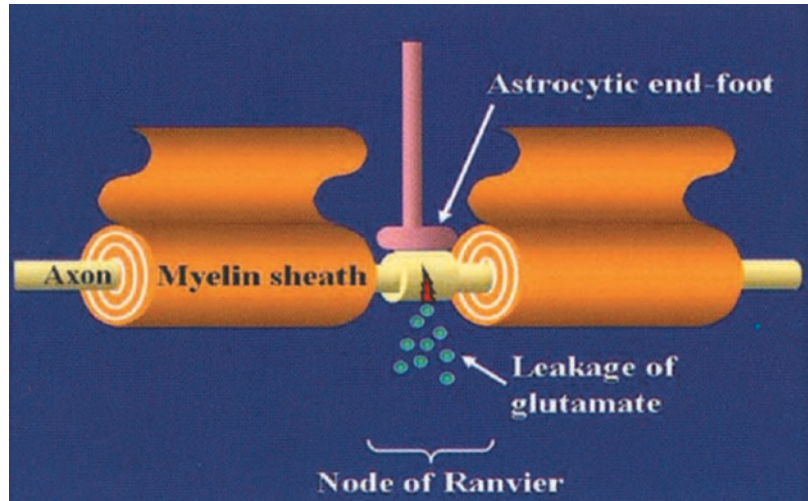
calcium ions, as in brain ischemia, which leads to axonal and glial cell swelling (cytotoxic or neurotoxic edema). These changes can eventually lead to axonal degeneration or necrosis with microglial and astrocytic reactive changes. Accumulation of hemosiderin-laden macrophages is also seen in the chronic phase. Glutamate is the most important excitatory amino acid and is responsible for many neurological functions such as cognition, memory, movement, and sensation. Glutamate mediates neuronal death in pathological conditions through the activation of NMDA receptor subtypes [33].

Cytotoxic edema, which seems to be the cause of reduced ADC in ischemic brain injury, can also occur in the early phase of DAI. However, reduced ADC is presumably due to the development of retraction balls and concomitant cytoskeletal collapse along the severed axons [25]. The time course of the ADC abnormality seems to be different from that of ischemic brain injury. Prolonged decrease in ADC, over 2 weeks, has occasionally been observed in DAI [26], and cytotoxic edema in the corpus callosum can be partially reversible on follow-up imaging using T2-weighted sequences. Axonal and glial cell swelling in DAI is thought to be mainly due to excitotoxic mechanisms that essentially propagates through the white matter tracts. It can also be a slower or reversible form of cellular swelling than that seen in ischemic brain injuries [18, 27,

28]. Hemorrhagic components, which often accompany these brain injuries, will affect the signal intensity on DW images.

The lesions with RD are usually not reversible; however, lesions with increased diffusion are partially reversible. A few isolated case reports of reversible intramyelinic white matter cytotoxic edema have been reported in traumatic brain injury patients [29].

DWI can also detect some hemorrhagic lesions but is not as sensitive as GRE or SWI (Fig. 17.9). The acute hemorrhagic foci which contain oxyhemoglobin are bright on DWI but dark on ADC and have a surrounding halo of increased diffusion because of vasogenic edema (Fig. 17.12 and 17.13). The hemorrhagic lesions then turn hypointense on DWI when they have deoxyhemoglobin, intracellular methemoglobin, or hemosiderin. Analysis of DWI and ADC data are less reliable in the presence of blood products [34, 35]. Moreover, the areas of the brain near the skull base, petrous pyramids, sphenoid, and frontal sinuses usually generate susceptibility artifact and may lead to false-positive or false-negative detection of lesions.

DWI images are helpful in predicting enlargement of the areas of hemorrhage seen on the initial CT scan after mild to moderate TBI. A study conducted by Kin et al. in Japan on trauma patients comparing CT and DWI MRI done in the acute phase of trauma patients found that the
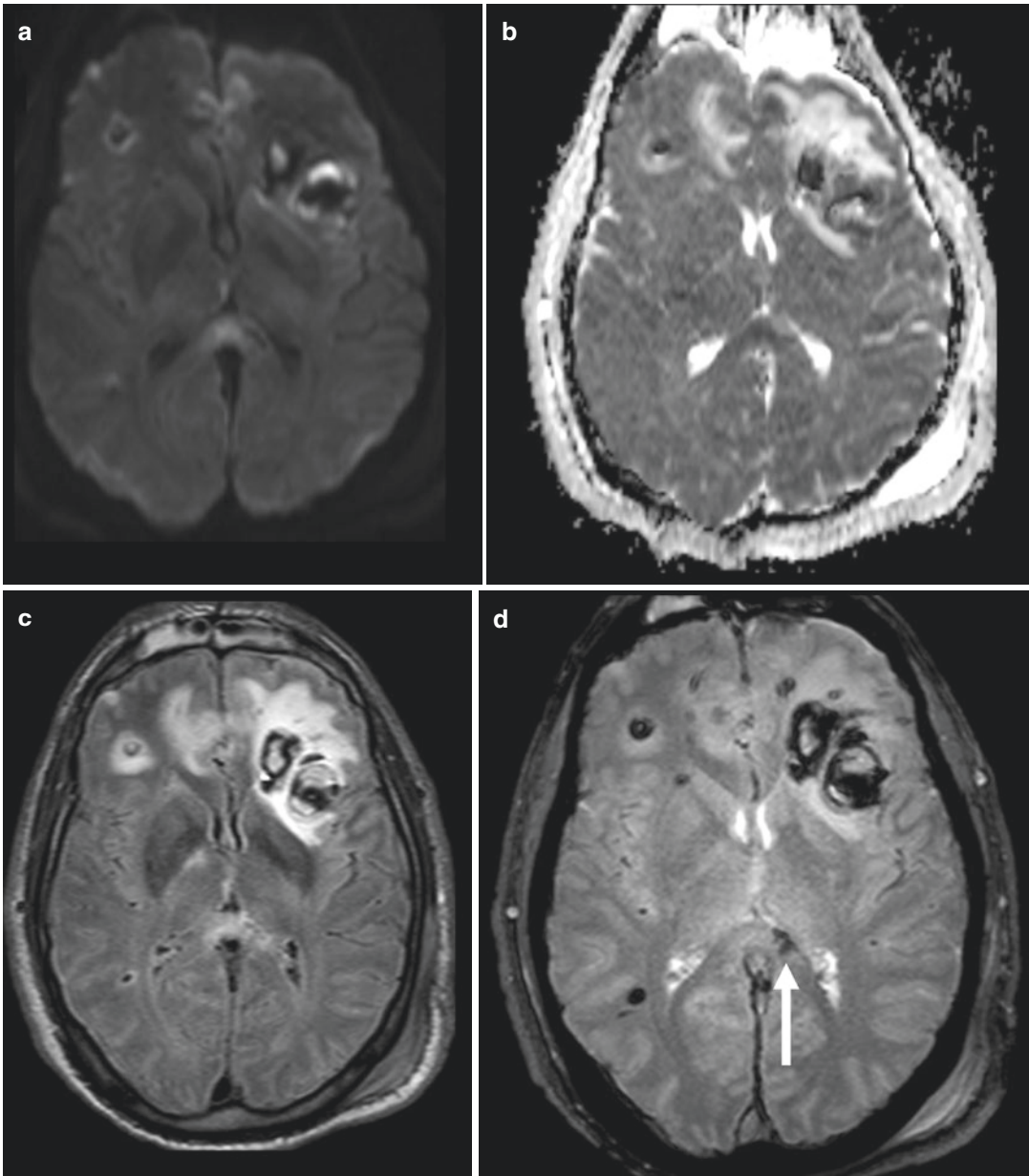
Fig. 17.12 (**a–d**) 22-year-old female with high-speed MVA shows multiple hemorrhagic contusions in bilateral frontal and right temporal lobes and DAI involving the splenium of corpus callosum. DWI (**a**) shows RD in the splenium of corpus callosum and multiple hemorrhagic contusions. ADC (**b**) shows dark SI in the splenium sug-gestive of RD. FLAIR (**c**) and GRE (**d**) images show the DAI lesion in the splenium of corpus callosum has both hemorrhagic (*arrow* on **d**) and nonhemorrhagic compo-nents. The hemorrhagic component on the left side is bet-ter seen on GRE and nonhemorrhagic component in the midline is better perceived on the DWI (**a**)

patients having a larger region of diffusion restriction compared to the size of initial hemor-rhage on the CT scan have a 71.4% chance of increase in the size of hemorrhagic lesions on the follow-up CT scans. Only 3% of the patients without a mismatch showed increase in the size of the hemorrhagic lesions. The fact that CT and MRI were performed at the same time makes this
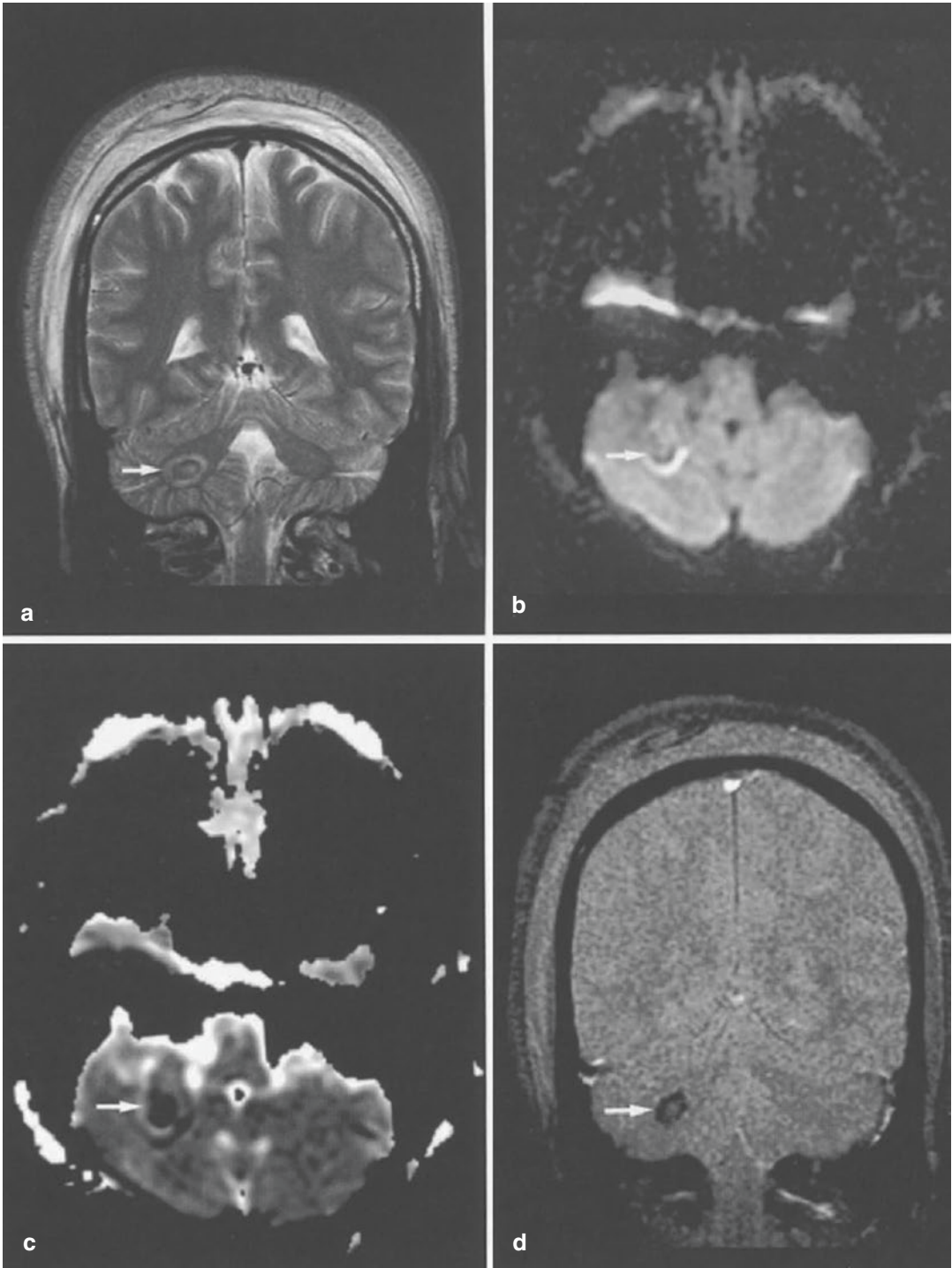
Fig. 17.13 (**a**–**d**) Diffuse axonal injury in the cerebellum of an 18-year-old male patient after a motor vehicle accident. (**a**) T2-weighted image shows a hypointense lesion in the right middle cerebellar peduncle (*arrow*), (**b**) DW image shows a hypointense lesion with a hyperintense rim, representing a hemorrhagic lesion (*arrow*). (**c**) ADC map reveals decreased ADC in this lesion (*arrow*). This may be due to a paramagnetic susceptibility artifact. (**d**) Coronal GRE image clearly demonstrates hemorrhagic lesions as hypointense (*arrow*)

study unique. The authors called this finding CT-DWI mismatch and hypothesized that these patients developed cytotoxic edema at the time of injury, and subsequent vasodilation increased the areas of hemorrhage. Therefore, the DWI may have an impact in management of the patients and decision-making during treatment [36].

Moen et al. conducted a longitudinal study to see the evolution of the DAI lesions in patients with moderate and severe TBI. They found that many nonhemorrhagic DAI lesions seen on FLAIR decrease in size and number in the scans performed after three months when compared to initial scans. The hemorrhagic lesions on GRE attenuated at a slower pace and did so after three months. MRI is the modality of choice for evaluating sequelae of TBI in subacute to late phases. However, MRI when performed earlier after injury provides better prognostic information and outcome. They found more lesions on FLAIR images as compared to DWI in the initial MRI scans, probably because half of the MRI scans were performed after 7 days of trauma [37]. However, more lesions were detected on the DWI as compared to FLAIR/T2 when MRI was performed within 48 hours of trauma in a different study [20]. They detected 310 shear lesions on DWI and only 248 shear lesions on FLAIR/T2. 65% of the lesions seen on DWI had restricted diffusion.

DWI is excellent in detecting the nonhemorrhagic lesions of DAI and the lesion load correlates well with the initial GCS and duration of coma in these patients. Multiple lesions are predictive of poorer outcome and lesion load in the corpus callosum has been confirmed by multiple studies to correlate with poorer outcome. However, the timing of the scan is important, as the lesion conspicuity and number on DWI decreases as time passes.

DWI is comparable to FLAIR in the detection of nonhemorrhagic DAI lesions [38, 39]. However, the GRE sequence is better in detecting the hemorrhagic lesions and SWI is even more sensitive and can detect a greater number of hemorrhagic lesions (Fig. 17.9). In a study conducted by Bansal et al., they detected a mean number of 7.47 lesions on DWI, 13.27 lesions on GRE, and 22.13 lesions on SWI. SWI has been found to detect 3–6 times more lesions as compared to GRE because it uses the magnetic susceptibility difference in the tissues resulting in phase difference between the paramagnetic deoxygenated blood products and surrounding normal tissues [22, 23]. However, there was no difference in the grading of DAI between the three sequences. Specifically, the grade of injury including involvement of the brainstem carries a poorer prognosis as compared to number of lesions in the hemispheric white matter [38, 40].

Huisman et al. found that DWI found the maximum number and overall volume of lesions in the brain in patients with DAI as compared to T2, FLAIR, and GRE sequences [20]. Schaefer et al. found that the larger volume of the DWI abnormalities in the brain in DAI cases have the highest correlation with GCS score at admission and with subacute Rankin scale score [27]. They also found a statistically significant correlation between reduction in the FA values in the posterior limb of the internal capsule and splenium of the corpus callosum and the severity of head injury measured by GCS score and Frankin score at discharge [20].

The modified Rankin scale measures the degree of disability and dependency in daily life after neurological injuries. The overall volume of the abnormal signal intensities on the DWI images has been found to have the strongest correlation with the modified Rankin scale at discharge in one study. A study found that lesion numbers seen on all sequences also strongly correlated with the modified Rankin scale. They found that location of lesions in the corpus callosum also had a strong correlation with this scale [27].

Hou et al. concluded that quantitative ADC measurements in different parts of the brain can be used to detect non-visible DAI and this information can be used to predict severity of injury and long-term outcome in trauma patients. They compared 37 trauma patients with 35 controls who had no brain injury. Mean ADC values in areas without visible DAI

lesions were significantly different from the normal controls. The patients with unfavorable outcomes had significantly higher ADC values as compared to patients with favorable outcomes and normal controls. They concluded, therefore, that ADC maps can be used to detect non-visible lesions [41].

MR has a value in prognostication as a larger number of DAI lesions seen on DWI predicts poorer outcome and more disability. The initial GCS, age, number of DAI lesions, and ADC scores can predict the duration of a coma according to a study conducted on 74 trauma patients. They found that advanced age, higher number of lesions, higher ADC values, and lower GCS scores predict longer periods of unconsciousness and poor prognosis [42].

## 17.6	Pediatric Patients

A study was conducted to evaluate the role of DWI in infants and toddlers with shaken baby syndrome (SBS), also called nonaccidental trauma. All 26 children enrolled in the study had SDHs, 18 cases of which were confirmed to have SBS. All of these 18 cases had DWI abnormalities in the brain and the lesions were larger on DWI compared to other MR pulse sequences. Most of these patients had SDHs, retinal hemorrhages, and fractures. Traumatic axonal injuries are also seen in these patients which are much better seen on MRI as compared to CT. Hence, the American Association of Pediatrics recommends an MRI when the medical condition is not explained by the CT findings alone (Fig. 17.14) [43].

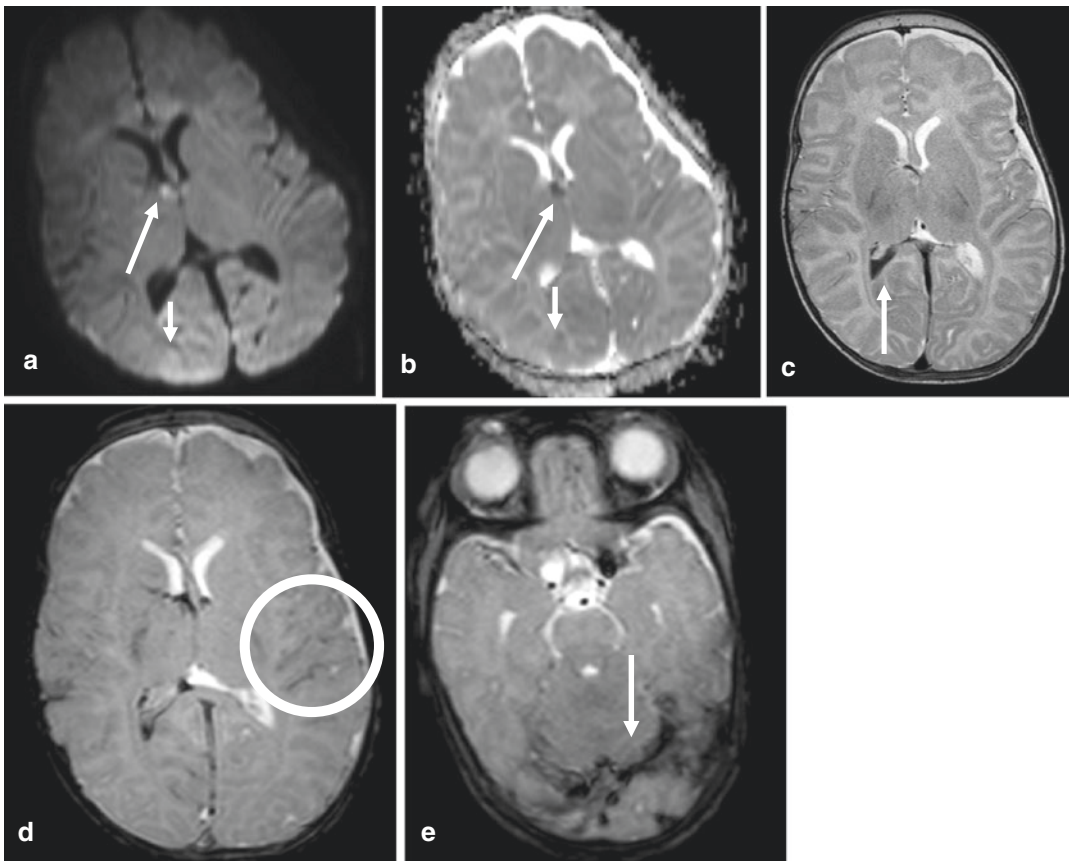**Fig. 17.14** (**a**–**e**) Four-month-old male child after nonaccidental trauma shows DAI with RD in the fornix (**a** is DWI and **b** is ADC) and IVH (**c** is T2 and **d** is GRE) and SDH (**e** is GRE) along the tentorium due to shaken baby syndrome. Mild RD in right occipital lobe is also seen (short arrow in **a**). Very subtle SAH is seen on the GRE in temporal lobes (circle in **d**)

A study was conducted on pediatric trauma patients and found that ADC values have prognostic significance in that lower ADC values in the peripheral white matter predict poorer outcome. The peripheral white matter had reduced ADC values in patients with severe TBI and poor outcomes when compared to patients with severe injury who experienced a relatively good outcome. They also concluded that average whole brain ADC values can predict clinical outcome in the trauma patients [40].

17.7 Hypoxic Ischemic Injuries

Hypoxic ischemic injuries (HII) in neonates can also cause RD on DWI in the brain. Areas of RD can be seen in the corpus callosum, basal ganglia, ventrolateral thalami, periventricular white matter, and/or peri-rolandic cortex depending on the gestational age, severity, and duration of the ischemic insult. Epelman et al. found that RD in the corpus callosum is more common than previously thought when neonates with suspected HII are scanned within the first week of age as pseudonormalization of RD happens earlier in the neonates [44].

17.8 Cerebral Fat Embolism (CFE)

Fat emboli to the brain is a rare entity which occurs after severe trauma when multiple long bone fractures lead to transfer of bone marrow fat into the systemic and pulmonary circulation by an unknown mechanism. This may lead to either generalized encephalopathy or focal neurological symptoms. This process should be suspected when there is altered mental status after a period of post-traumatic normal mental function in a patient with long bone fractures or after orthopedic fixation of long bone fractures [45]. CT is very insensitive and usually misses the findings. MRI generally shows patchy or confluent areas of vasogenic and cytotoxic edema in the deep white matter, basal ganglia, cerebellum, and corpus callosum. This is better seen on GRE or SWI as a diffuse pattern of multiple lesions with micro-susceptibility artifacts because of vascular stasis, deoxygenated blood, and microthrombi formation, as well as larger areas of restricted diffusion (Fig. 17.15) [2, 46, 47].

Appearance of lesions 2–3 days after injury in a diffuse and symmetrical manner in addition to involvement of the cerebellum favors fat emboli over TAI. The DWI and T2* are helpful to distinguish fat embolism from DAI. Diffuse confluent larger lesions with restricted diffusion and a greater number of small hemorrhages are seen in CFE, while larger or more linear hemorrhages and fewer number of scattered foci of RD are more typical of DAI [46]. The prognosis is generally worse for DAI.

17.9 Traumatic Optic Neuropathy (TON)

DWI has high specificity for diagnosing traumatic optic neuropathy in patients with the appropriate clinical setting. TON is usually a clinical diagnosis, but in some comatose or otherwise difficult to examine patients, MRI can be very helpful. Specifically, identification of RD in the optic nerve can indicate traumatic contusion and ischemia and has been shown to have 27.6% sensitivity and 100% specificity in the diagnosis TON (Fig. 17.16) [48]. One of the reasons for low sensitivity in their study may be the use of 5 mm slices for DWI; use of 3 mm slices may increase the sensitivity of MR for TON. The presence of high signal intensity on DWI is useful to diagnose TON, but absence of RD in the optic nerve has lesser negative predictive value, in that the optic nerves may not be well seen because of motion or susceptibility artifacts. RD tended to be seen in the posterior segment of the optic nerves in this study which may be due to increased vulnerability of the nerve in or near the optic canal and the potential for compartment syndrome.
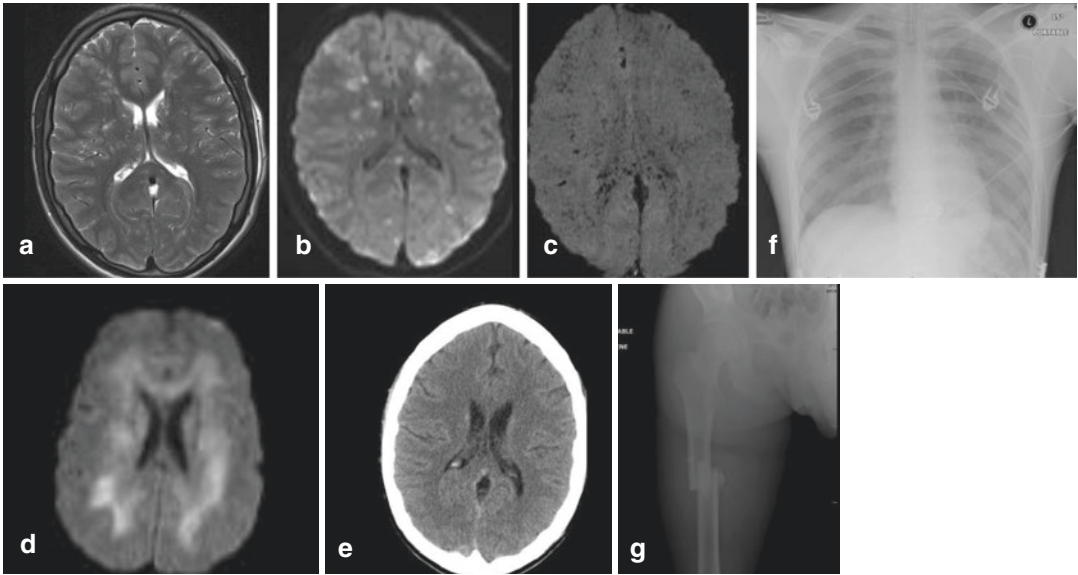
Fig. 17.15 (**a–g**) 19-year-old man with MVA. T2WI (**a**) and DWI (**b**) show starfield pattern of lesions associated with numerous micro-hemorrhages on susceptibility-weighted image (**c**). 7-day follow-up DWI (**d**) shows diffuse white matter changes. 2 months follow-up CT (**e**) demonstrates reversibility of the edema. Cerebral fat embolism syndrome occurs in 2–5% of long bone fractures (**g**). It is also associated with sickle cell disease, pancreatitis, and liposuction. Fat emboli and/or toxic free fatty acids which disrupt capillary endothelium are the cause of the syndrome and pulmonary edema (**f**). Reversible diffuse white matter changes can be seen during the course of the syndrome
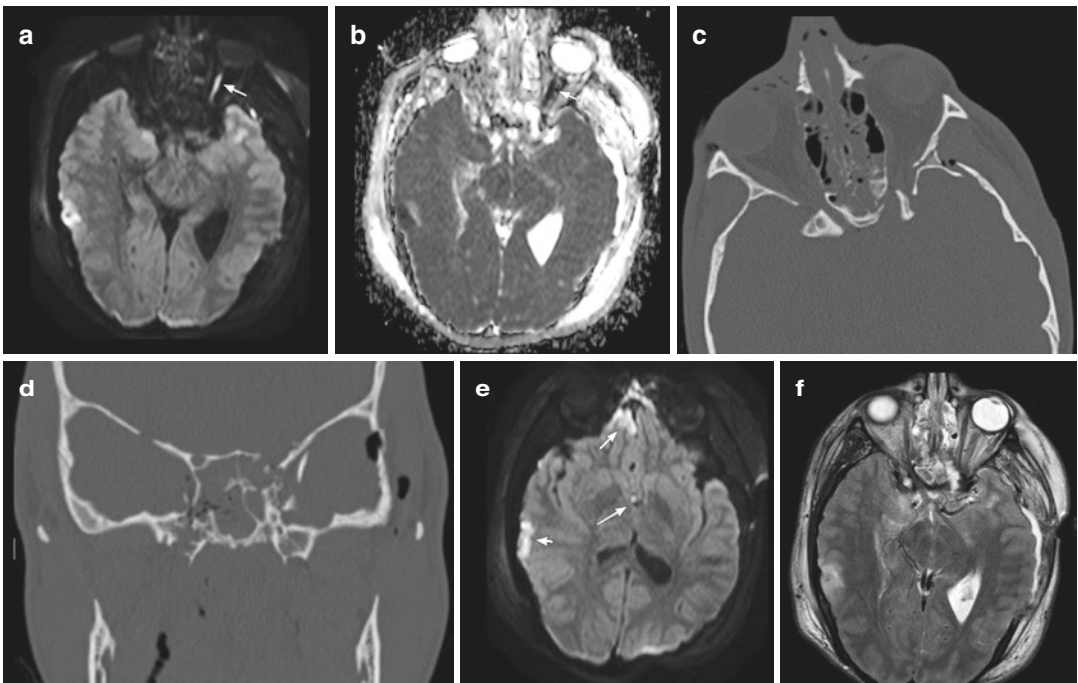

Fig. 17.16 (**a–f**) 18-year-old male after MVC and loss of vision in left eye. DWI (Image **a**) shows RD in the left optic nerve and shows hypointensity on the ADC maps (**b**) suggestive of optic nerve injury which was due to multiple fractures around the left orbital apex and optic nerve canal (**c**, **d**). DAI in the fornix (arrow in **e**) with multiple contusions in frontal and temporal lobes (**e**) are also seen. T2 (**f**) shows subtle hyperintensity and swelling of the left optic nerve

17.10 DWI in Mild Traumatic Brain Injuries (mTBI)

70–90% of all hospital-treated injuries are mild with an incidence of approximately 300 in 100,000 [33]. These lesions are greatly underdiagnosed as they are not seen on the CT scan and even on routine MRI pulse sequences. Very few trauma patients with mild injuries receive MRI of the head. Many of these patients will suffer long-term cognitive deficits. Common issues of cognitive impairment suffered by these patients after mTBI are memory, information processing speed, attention, and executive function. DWI and DTI have been shown to detect cases of mTBI [49, 50].

DWI is a sensitive technique to detect DAI as it can evaluate structural integrity of the white matter tracts [25, 51], even in patients with mild traumatic brain injuries (mTBI). mTBI is defined as patients with GCS > or equal to 13. 70 to 90% of the patients with traumatic brain injuries have only mTBI [2, 52]. Many studies have been performed confirming structural damage to the white matter tracts in some patients after mTBI which is not seen on conventional MRI.

17.11 Diffusion Tensor Imaging (DTI) and Fractional Anisotropy (FA)

Diffusion tensor imaging (DTI) is a robust tool to detect mild DAI and is superior to conventional MRI. DTI is derived from directionally encoded diffusion-weighted data by obtaining diffusion parameters in multiple (minimum six but usually many more) non-collinear planes and post processing the data set to produce three-dimensional white matter tracts. DTI measures directional diffusion of water molecules in the white matter tracts. The diffusivity of water in CSF and in the gray matter is isotropic, as it can equally move in all directions without any hindrance or preference. The diffusivity of the water molecules in the white matter tracts is anisotropic, which means that water molecules cannot move equally in all directions. The diffusivity is maximum along the direction of the white matter tract and this phe-

nomenon is called fractional anisotropy (FA), which can be measured. The FA of CSF in the ventricles and FA of gray matter is close to zero and FA of large white matter tracts in the corpus callosum is close to one. DTI data when combined with post-processing techniques can generate diffusion tensor tractography maps which show the three-dimensional anatomy of the white matter tracts [53–55].

Fractional anisotropy is the main quantitative metric obtained from DTI and measures anisotropic diffusion. Higher FA means homogeneity in fiber orientation, increased fiber density and axonal diameter. Reduced FA in white matter indicates damage to myelin, damage to axon membranes, a reduced number of axons, increased edema, or decreased axonal coherence [33, 56, 57]. DTI imaging can show two different patterns of the early phase of DAI: (1) decreased FA with decreased or isointense ADC which represents mixed intra- and extracellular edema and broken fibers, and (2) normal FA with decreased ADC which represents pure cytotoxic edema and presumably preserved fiber connectivity (Figs. 17.17 and 17.18). In the late phase of DAI, decreased FA and increased ADC are observed. DT imaging is thought to be useful in the early detection of DAI and a prognostic measure of subsequent brain damage [56].

Many studies have found changes in FA in patients with mTBI in both acute and chronic phases. Most reports are consistent in the finding of reduced FA during the chronic phase (>2 weeks) [33, 58]. However, the literature varies in the FA values in the acute phase after mTBI and they may be increased or decreased. Eierud and colleagues published a meta-analysis in 2014 after reviewing 122 publications on DTI and mTBI and found that increased FA was reported more frequently than decreased FA in acute settings [59]. This increased FA in acute settings may be due to axonal injury in areas of crossing fibers and markedly reduced extracellular diffusivity in the setting of cytotoxic edema [33].

The FA is reduced, and diffusivity is increased in cases of moderate to severe TBI and several studies have validated this observation in adult and pediatric patients [11, 25, 60]. The degree of reduction of FA also correlates with TBI severity [61].
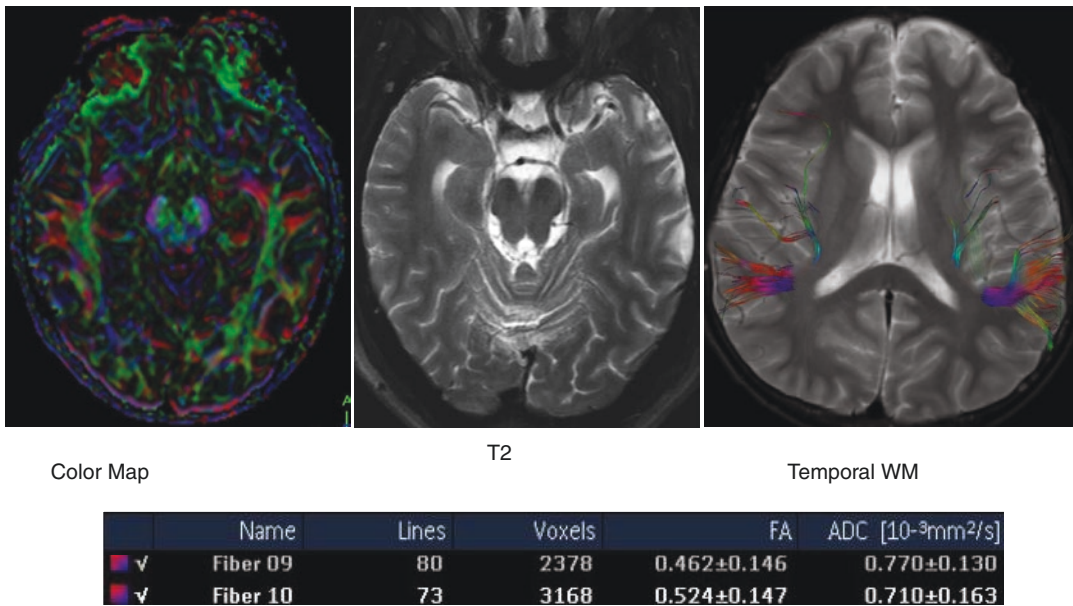
	Name	Lines	Voxels	FA	ADC [10⁻³mm²/s]
■ √	Fiber 09	80	2378	0.462±0.146	0.770±0.130
■ √	Fiber 10	73	3168	0.524±0.147	0.710±0.163

Fig. 17.17 16-year-old male suffering from Post-Concussion syndrome after TBI after MVA shows decreased FA and increased diffusivity in the left temporal lobe. (Case Courtesy by Dr. Gaurang Shah)

Axial diffusivity (AD) and radial diffusivity (RD) are other DTI metrics. AD, also called longitudinal diffusivity, is the diffusivity along the fastest direction of diffusion which is invariably along the long axis of the fiber tract and is affected by the pathologies of the axons. RD, also called transverse diffusivity, measures the diffusivity perpendicular to the fiber tract and is affected by the pathologies of the myelin [62]. The AD and RD show different patterns of increased or decreased values based on the severity of injury and time since injury.

Those patients who suffer from post-concussion syndrome (PCS) after mTBI have more structural impairment as compared to the patients of mTBI without PCS. A study was conducted on 53 patients with mTBI and 40 healthy volunteers. The DWI was performed on a 3 T magnet in 50 non-collinear gradient directions in the subacute and late phases of the injury. They discovered that patients with PCS had decreased fractional anisotropy (FA) and increased mean and axial diffusivity in association, projection, and commissural white matter tracts [63].

Many studies have cross-validated DTI detection of DAI by using microdialysis of CSF, where reduction in the FA correlated to interstitial fluid tau levels. Tau is a structural protein of axons and increased levels in CSF are seen after TBI [11, 64].

The deterioration of white matter tracts continues for up to 2 years after initial injury according to numerous investigations [60, 65]. Many studies have seen continuous measurable deterioration in the white matter integrity parameters after the initial insult and linked this to ongoing microstructural changes which continue after initial injury. The authors suggested that there is delayed activation of complex intracellular biochemical cascades after initial injury which lead to axonal transection called secondary axotomy and may be the cause of progressive clinical decline after initial trauma [11].

DTI evaluation of the corpus callosum is superior to smaller white matter tracts because of the large size of the bundle and unidirectional orientation of tracts in the corpus callosum. However, DTI cannot resolve crossing fibers as well, and FA is usually decreased in regions of crossing
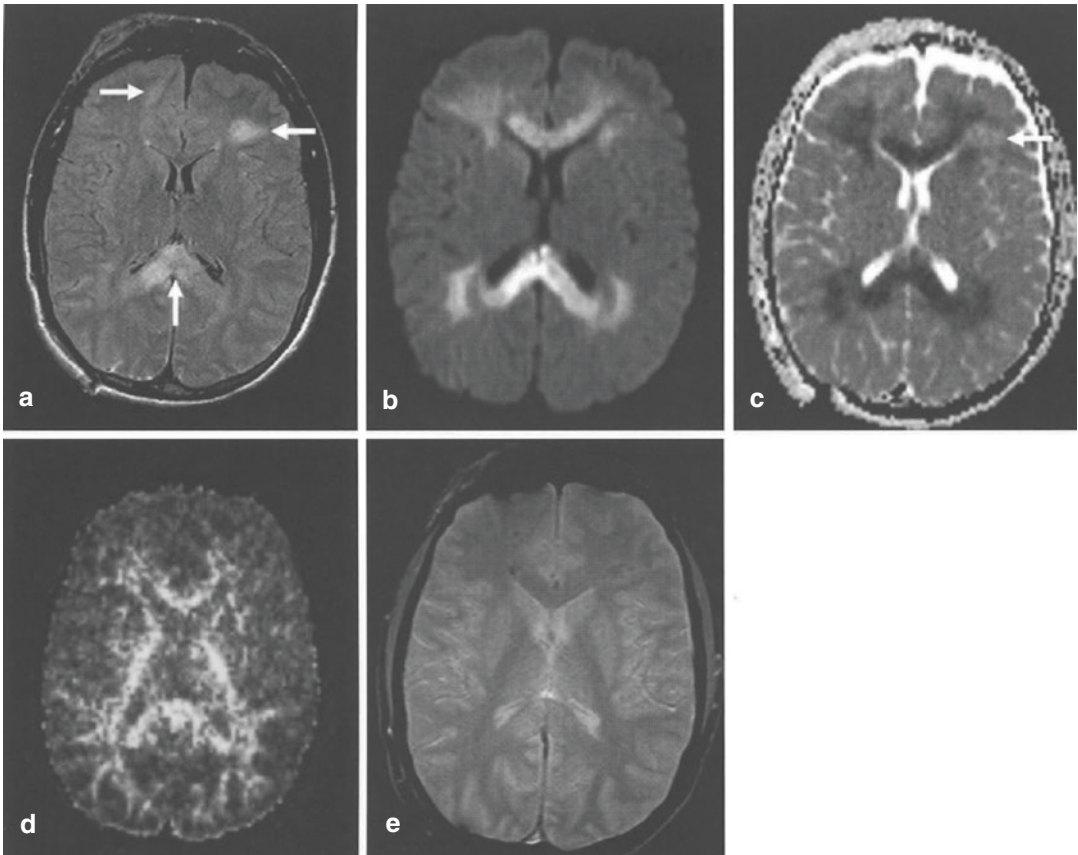
Fig. 17.18 (**a**–**e**) Diffuse axonal injury in a 24-year-old man after a motor vehicle accident. (**a**) FLAIR image shows multiple asymmetric hyperintense lesions in the bilateral frontal white matter and the corpus callosum (*arrows*). (**b**) DW image shows diffuse hyperintense lesion in the deep white matter and the corpus callosum. (**c**) ADC map reveals decreased ADC in the deep white matter and the corpus callosum. The left frontal lesion seen on FLAIR image has iso- to slightly increased ADC (*arrow*). (**d**) FA is preserved in most of the diffuse white matter abnormalities suggestive of a pure cytotoxic edema. Decreased FAs are observed in the lesions in the bilateral frontal white matter and splenium of the corpus callosum seen on the FLAIR image. (**e**) GRE image demonstrates hemorrhagic foci in the frontal white matter

fibers which makes it difficult to evaluate the areas of brain where white matter tracts are crossing [66]. The changes in the metrics of DTI and FA are not specific to DAI and can be seen in a wide variety of white matter disorders.

Multiple studies have documented that many patients of mTBI who had no radiological evidence of trauma in the brain, and who then died from other causes, had microscopic diffuse axonal injuries on autopsy [6, 62]. Yuh and colleagues conducted a study on mTBI patients and concluded that the prognostic utility of DTI is better than CT, clinical, or demographic socioeconomic variables in the prediction of 3- and 6-month outcome [67].

However, there are many limitations including high cost, MRI safety issues, medical stability of the polytraumatism patients, variable protocols, lack of standardized metrics, post-processing techniques, and lack of correlation with clinical findings which impede routine use of DTI for TBI patients [11].

17.12 Diffusion Kurtosis Imaging (DKI)

Diffusion kurtosis imaging uses multishell imaging with numerous b-values of more than 1000 s/mm^2 to quantify the non-Gaussian behavior of diffusion. The diffusion images have a Gaussian behavior when b values are equal or less than 1000 s/mm^2 and it becomes non-Gaussian at values above b-1000. Kurtosis is a measure of the deviation from a Gaussian distribution and depicts tissue microstructure complexity. This technique can detect subtle injuries even in areas where FA is low [62, 66, 68].

17.13 DWI Thermometry

DWI thermometry is a novel research technique which can measure brain core temperature using DWI data, calculations, and the principles of kinetic theory. The diffusion coefficient of the non-restricted water molecules in the lateral ventricles can be measured which can help to calculate the temperature [69]. Tazoe et al. conducted a study in 2014 which measured brain core temperatures in patients with mTBI and found that they were reduced, which may be due to a global decrease in metabolism or perfusion or both [70]. However, brain temperature increased after moderate to severe TBI due to increased intracranial pressure and higher resistance to blood flow.

17.14 DWI and Cognition

Conventional imaging findings in mTBI do not predict the neurocognitive outcome. However, Miles and colleagues found a positive correlation between low FA and poor executive functions [71]. In a different study, global burden of the injuries in mTBI as measured by DTI correlated with a decline in executive function and cognitive processing speed [51]. The volume and total number of traumatic lesions on DWI (whether facilitated or restricted diffusion) in the acute phase of head injury has shown strong correlation with memory deficits in patients with mild trau-

matic injuries and with modified Rankin scale in moderate to severe trauma [27, 72].

17.15 DWI in Focal Traumatic Lesions

CT is excellent in the initial evaluation of extradural and subdural hematomas, traumatic subarachnoid hemorrhage, parenchymal hematomas, brain contusions, fractures, and complications such as midline shift and herniation. However, MRI has its own advantages in certain situations and is more sensitive for subtle lesions.

17.16 Contusions

Brain contusions are defined as traumatic injuries to the cortical surface of the brain and are caused by direct impact by the skull to the brain and can be coup and/or countercoup injuries. They are most commonly seen in the inferior surface of the frontal lobes, anterior and inferior aspect of the temporal lobes, and lateral aspects of the brain due to impact from hard bony ridges of the skull base. Contusions are large, multiple, bilateral, more ill-defined, more likely to be hemorrhagic, and are seen in the superficial aspect of the brain (Figs. 17.12, 17.16, 17.19, 17.20, and 17.21). Cytotoxic edema in brain contusions is also related to excitotoxic mechanisms [73–75].

CT scan underestimates contusions especially when they are smaller and nonhemorrhagic. MRI is more sensitive in detecting these contusions and DWI shows that they are heterogeneous and have mixed areas of cytotoxic and vasogenic edema. Brain contusions can show an interesting appearance on DWI, with a core of low SI on diffusion and increased ADC surrounded by a rim of high SI on diffusion with decreased ADC. This happens because of disintegration and homogenization of the intra- and extracellular components in the central area, whereas cellular swelling is predominant in the peripheral areas [74].

Occasionally MR may be performed in such patients when there is unexplained neurological deficit and a mismatch between CT findings and
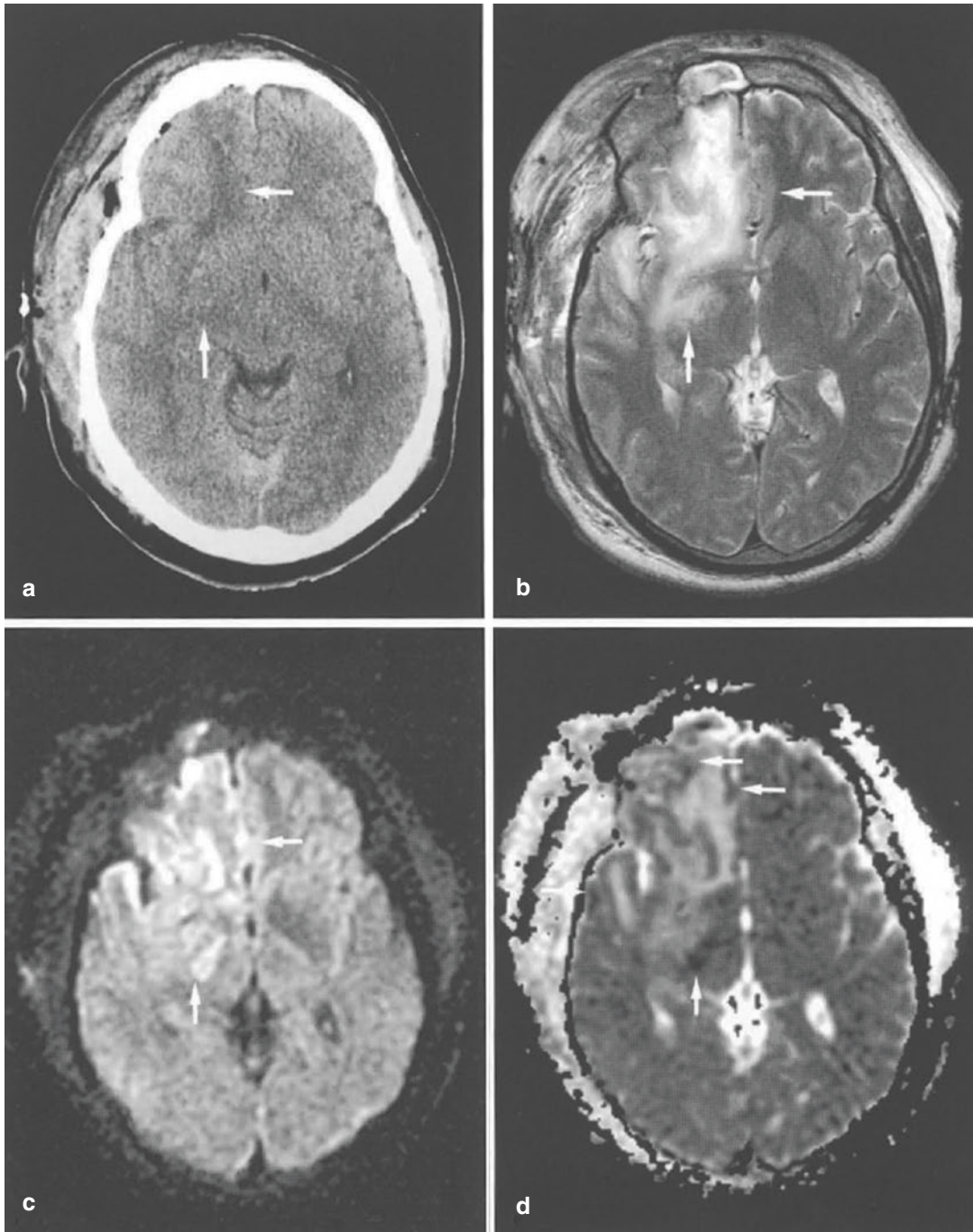
Fig. 17.19 (**a–d**) Brain contusion in the frontal lobe in a 37-year-old man after a motor vehicle accident. (**a**) On CT obtained after evacuation of epidural hematoma, it is difficult to delineate the extent of contusion in the right frontal lobe (*arrows*). (**b**) T2-weighted image delineates the extent of the edematous brain contusion (*arrows*). (**c**) DW image shows heterogeneous signal intensity in these lesions, representing mixed vasogenic and cytotoxic edema with hemorrhagic necrotic tissues (*arrows*). (**d**) ADC map reveals mixed increase and relative decrease of ADC (*arrows*) in these lesions
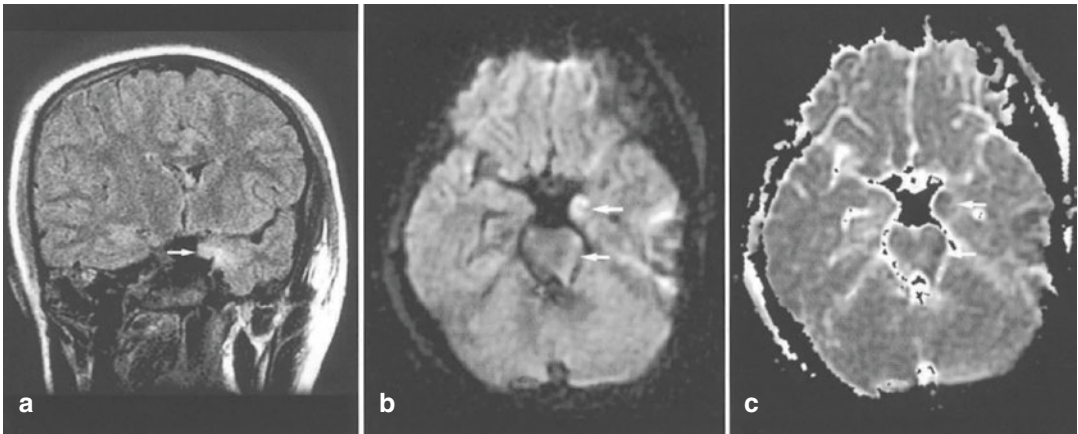
Fig. 17.20 (**a**–**c**) Brain contusion in the hippocampus in an 11-year-old girl after a motor vehicle accident. (**a**) FLAIR image shows a hyperintense lesion in the left hippocampus (*arrow*). (**b**) DW image shows this lesion as hyperintense. (**c**) ADC is decreased in the left hippocampus and left side of the brain stem (*arrows*), representing mainly cytotoxic edema
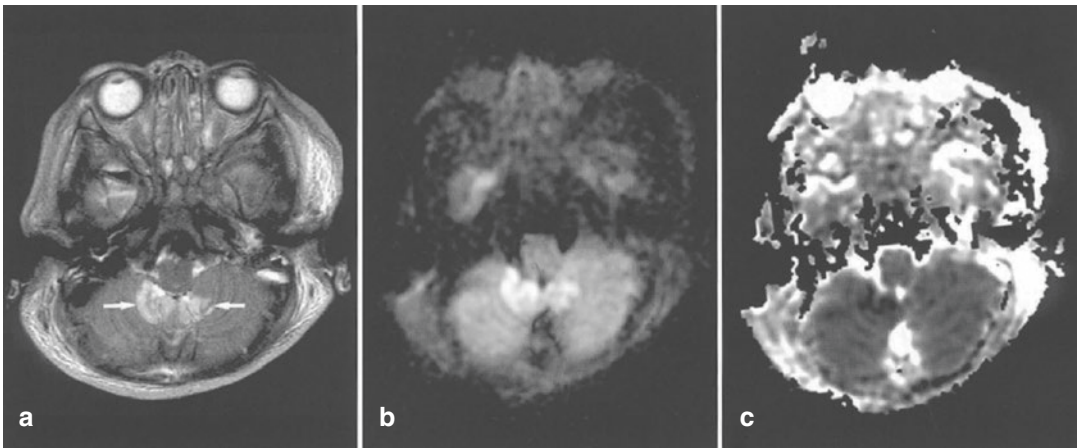

Fig. 17.21 (**a**–**c**) Brain contusion in the cerebellar tonsil in an 11-year-old girl after a motor vehicle accident. (**a**) T2-weighted image shows hyperintense lesions in the cerebellar tonsils (*arrows*). (**b**) DW image shows this lesion as hyperintense. (**c**) ADC is partially decreased

clinical examination. MR is more sensitive for detection of nonhemorrhagic contusions, especially when they are small. FLAIR and DWI will depict them as foci of abnormal signal intensity. DWI may show them as restricted or facilitated diffusion depending on various factors. Small hemorrhagic contusions are better seen on GRE and SWI sequences, with SWI 3–6 times more sensitive. Most institutions perform either GRE or SWI, as they serve the same purpose.

17.17 Extra-axial Hematoma

Traumatic hemorrhages result from injury to a cerebral vessel (artery, vein or capillary) [4]. Subdural hematomas originate from disruption of the bridging cortical veins, which are vulnerable to rapid stretching. Epidural hematoma can have either an arterial or a venous sinus origin, typically associated with a skull fracture. MR imaging is extremely helpful to detect hematomas,

especially along the vertex and skull base, and can in certain questionable cases differentiate between subdural and epidural hematomas [4, 76–79] (Figs. 17.22, 17.23, 17.24, and 17.27).
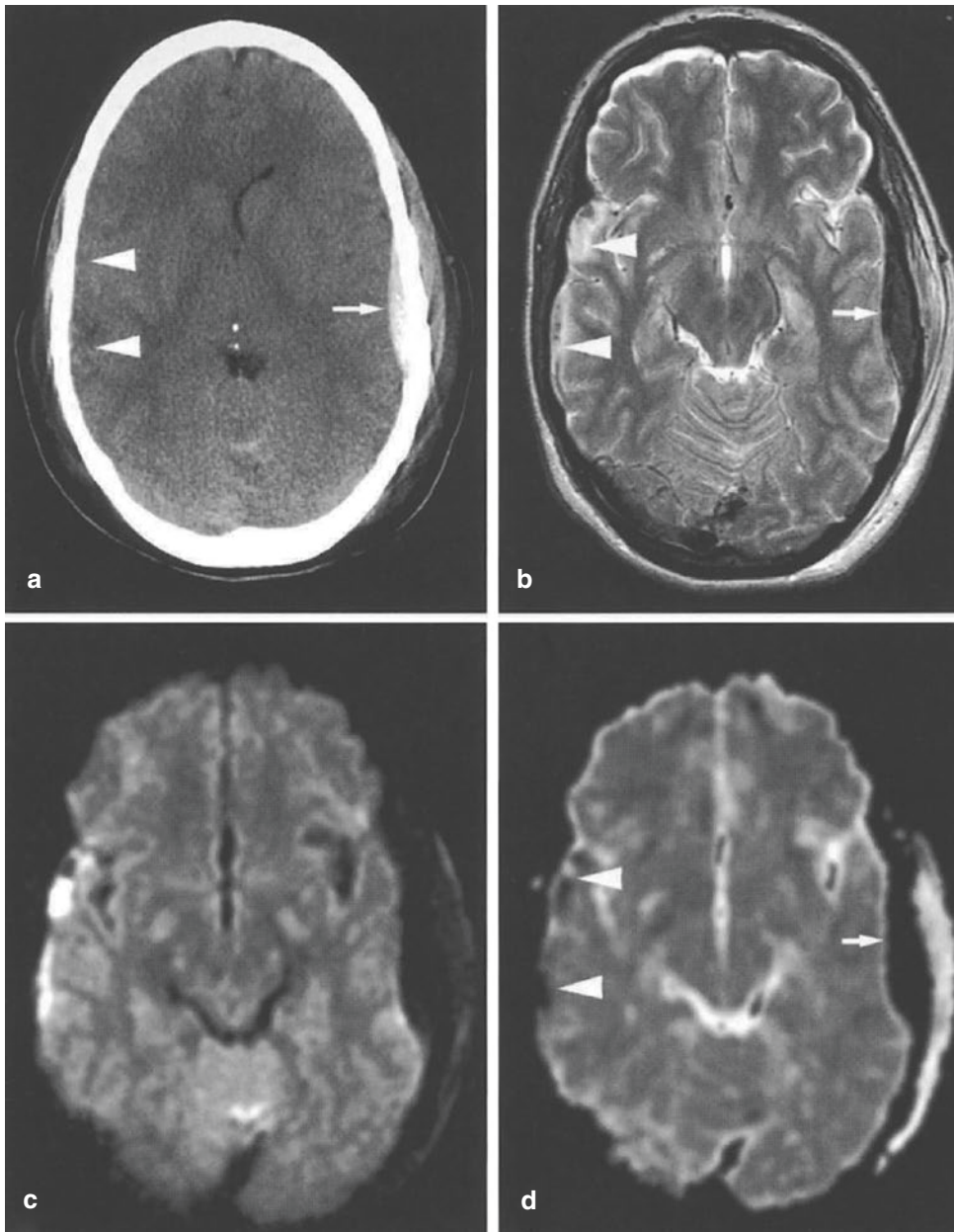

Fig. 17.22 (a–d) Epidural and subdural hematoma in a 26-year-old man after a motor vehicle accident. (**a**) CT shows a left epidural hematoma (*arrow*) but it is difficult to depict the isodense small subdural hematoma in the right side (*arrowheads*). (**b**) T2-weighted image shows the left epidural hematoma (*arrow*) as a hypointense lesion and the right subdural hematoma as partially hypointense lesions (*arrowheads*). (**c**) DW image shows the epidural hematoma as very hypointense due to deoxy-hemoglobin, and the subdural hematoma as very hyperintense presumably due to high viscosity or hypercellularity of hematoma. (**d**) ADC map shows hypointensity due to loss of pixels with background masking in the left epidural hematoma (*arrow*). ADC map also shows decreased ADC in the right subdural hematoma (*arrowheads*)

Very thin (1–2 mm thickness) SDH are better seen on MRI on T1-weighted images as thin curvilinear areas of hyperintensity due to methemoglobin formation. These can also be seen on FLAIR, DWI, T2, or GRE and will have different signal intensities based on the age of hemorrhage and other factors. MRI is more sensitive than CT for detecting these thin SDH because of high imaging contrast between hematoma and signal void of bone. However, subdural hematomas that are missed on CT are almost always very thin and of doubtful clinical significance. MRI can also help to predict the approximate age of the hematoma [2, 4, 8, 80] (Figs. 17.22, 17.23, and 17.27).
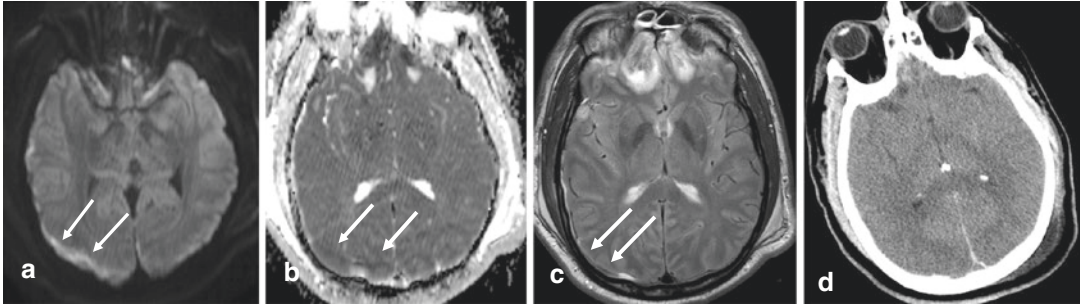

Fig. 17.23 (**a**–**d**) Acute subdural hematoma. 38-year-old male patient after fall from roof shows thin right convexity SDH as RD on DWI (**a**) and is difficult to see on the CT scan (**d**). DWI and other MR sequences (**b** is ADC and **c** is T2) are more sensitive for thin SDH because of better contrast resolution and signal void of the adjacent bone
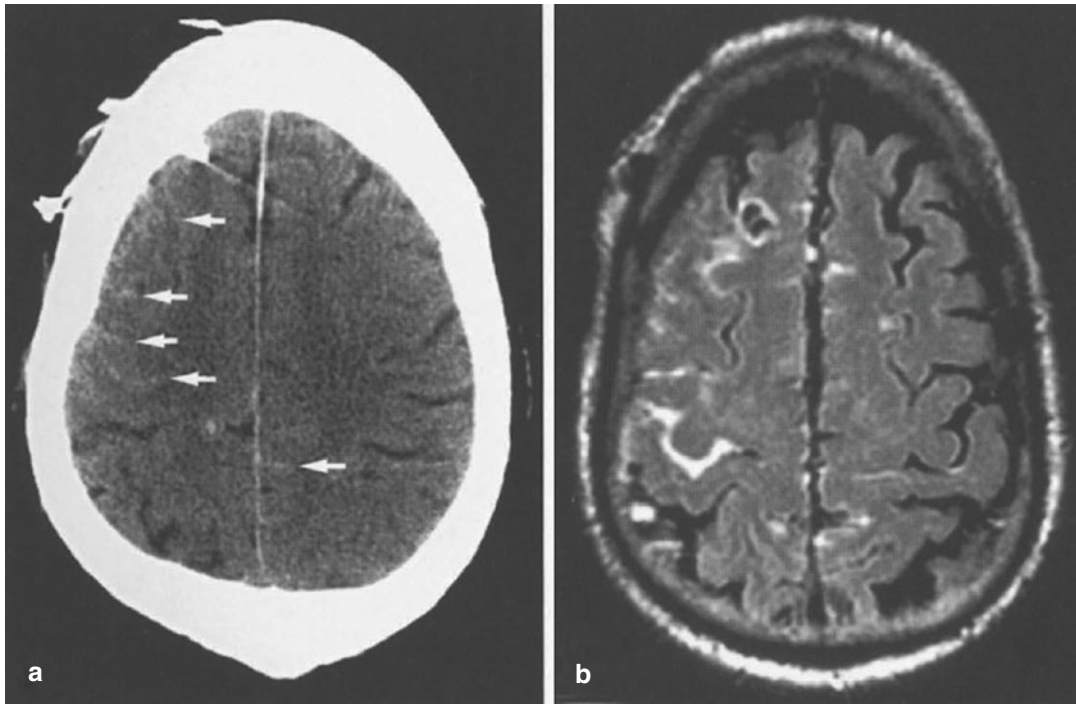
Fig. 17.24 (**a**–**d**) Subarachnoid hemorrhage in a 68-year-old man with ruptured aneurysm of the right middle cerebral artery bifurcation. (**a**) Postoperative CT shows subtle high density of subarachnoid space in the right frontoparietal area (*arrows*). (**b**) FLAIR image shows subarachnoid hemorrhage as hyperintensity. (**c**) DW image also shows subarachnoid hemorrhage as hyperintensity with mildly increased ADC (not shown). (**d**) Coronal GRE shows the hemorrhage as low signal intensity

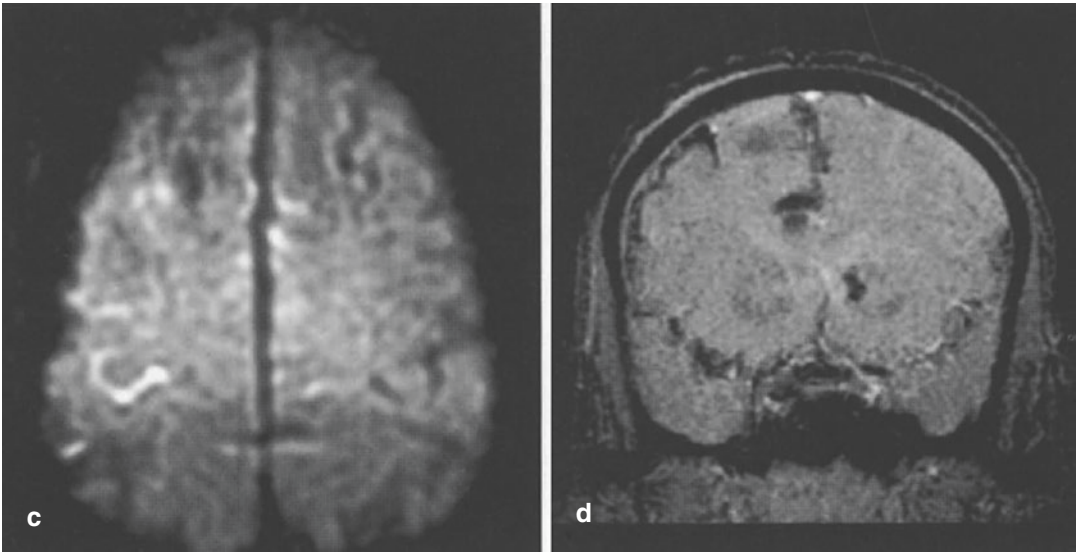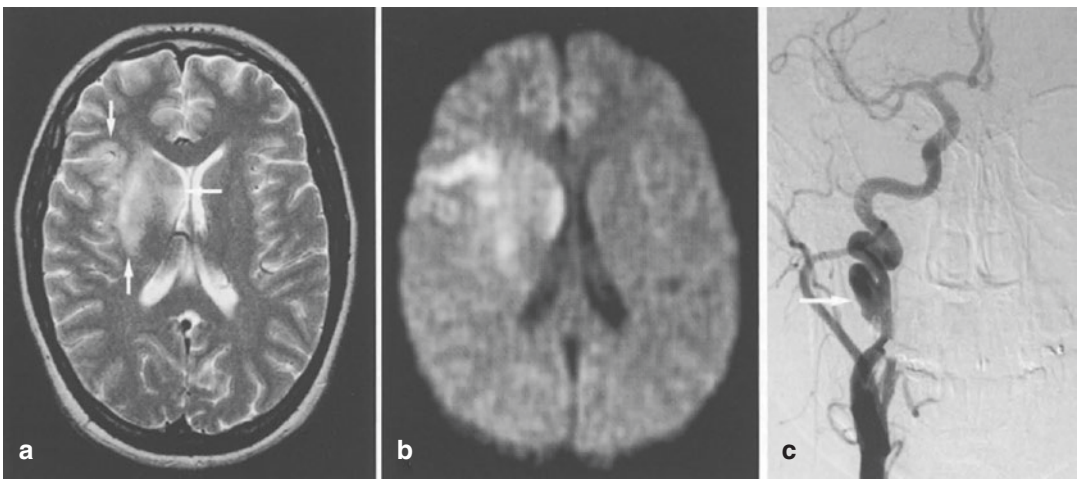**Fig. 17.25**   (**a**–**c**) Cerebral infarction after carotid artery dissection with pseudoaneurysm in a 20-year-old female patient after a motor vehicle accident. (**a**) T2-weighted image shows hyperintense lesions in the right middle cerebral artery territory including the right basal ganglia (*arrows*). (**b**) DW image also shows these lesions as hyperintense with decreased ADC (not shown), representing acute infarction. (**c**) Conventional angiogram shows pseudoaneurysm of the right carotid artery (*arrow*)

17.18 Diffusion in Vascular Injuries and Infarcts

Traumatic arterial and venous injuries (dissections, lacerations, occlusions, pseudoaneurysm, arteriovenous fistulas) are more prevalent than generally believed. Many asymptomatic lesions probably escape detection, and others are recognized several days to months after the injury (Fig. 17.25). Vertebral artery injuries are more common after blunt trauma, mainly due to fractures of the cervical spine, LeFort II and III facial fractures and skull base fractures. Carotid artery injuries are more common with penetrating

trauma. These injuries may cause dissection, occlusion, pseudoaneurysm, and other abnormalities which can lead to thromboembolism or obstruction of flow with resultant infarction. Fractures of the occipital and temporal bones and the skull vault may also predispose to dural sinus thrombosis leading to venous infarcts within a few days after the initial trauma [2, 31, 81].

CTA and CTV have high accuracy to detect vascular injuries and are the best initial tests to evaluate the arterial and venous structures whenever vascular injuries are suspected. MR head along with MRA or MRV can be performed for the evaluation of possible infarcts, or when iodinated contrast is contraindicated. Diffusion-weighted imaging is the most sensitive sequence for the detection of acute infarcts as it can show restricted diffusion within minutes of clinical onset.

Conventional angiography is still the gold standard in the diagnosis of vascular injuries but is usually reserved for neurointervention, problem-solving cases or in cases marred by metallic artifact after gunshot injury.

17.19 Diffusion in Secondary Injuries and Postoperative Complications

Prolonged and prominent midline shift because of large SDH or EDH can cause compression on the anterior and posterior cerebral arteries leading to infarcts. Descending transtentorial herniation can cause duret hemorrhages, contusions, and edema in the brainstem. DWI is extremely sensitive in picking up these findings of acute infarction and edema, if the patient is a candidate for an MRI [2, 4]. However, in many such cases, the patients are very sick and too unstable to undergo an MRI. CT head is then usually performed.

DWI is very sensitive and accurate for the diagnosis of hypoxic-ischemic brain injuries which may result from catastrophic cardiac or vascular problems. Restricted diffusion is seen in the affected areas which usually involve the cerebral cortex, cerebellar hemispheres, and basal ganglia [82].

Some patients develop intracranial infections after craniotomies and skull base fractures which cause persistent CSF leaks. These patients may develop subdural or extradural empyema, abscesses, or cerebritis. MRI brain with and without contrast is extremely valuable in such patients. Diffusion images show restricted diffusion within abscesses, as well as in empyema because of pus accumulation. However, hemorrhage in acute phases can also show restricted diffusion due to blood degradation products; hence these cases should be interpreted with caution. DWI has limitations in differentiating postoperative subdural empyema from hemorrhagic, noninfected fluid collections after intracranial surgeries and accuracy improves approximately three months after surgery [83]. One study found a 37% rate of false-positive DWI findings for infection in the postoperative period [84]. This was because noninfected hemorrhagic fluid collections due to craniotomies or subdural hematomas may show restricted diffusion in the acute to subacute stages. Evaluation of precontrast T1-weighted images is helpful as hemorrhagic fluid collections will be hyperintense. They also found that infections in extradural fluid collections are less likely to show restricted diffusion. The imaging appearance on all pulse sequences, comparison with all prior imaging studies, change in size and morphology with time, and clinical parameters should be carefully assessed to distinguish hemorrhagic fluid collections from empyema (Figs. 17.26 and 17.27).

17.20 Summary

TBI are very common and CT is the mainstay for the management and triage in the majority of these patients. However, MR plays a significant role in problem-solving cases when there is an unexplained neurological deficit not explained by the CT, or if certain complications are suspected. Injuries can be focal or diffuse and DAI is a diffuse injury which is often missed on CT. FLAIR,
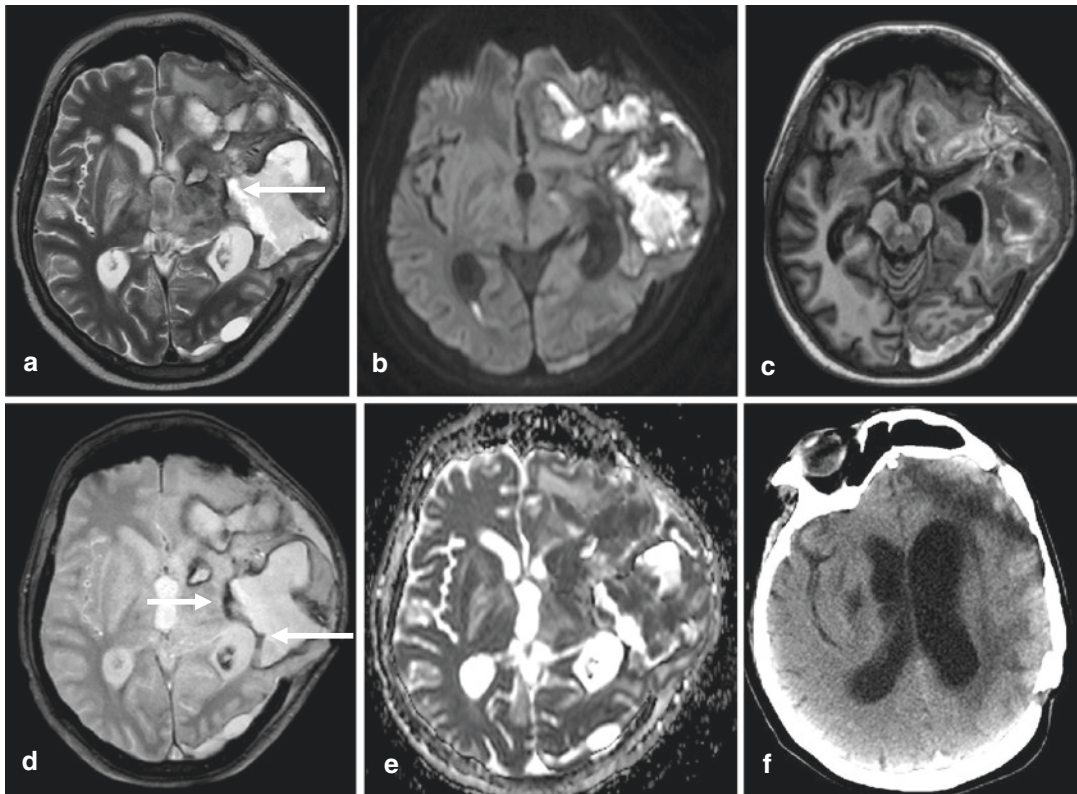
Fig. 17.26 (**a–f**) 46-year-old female patient with history of MVA and left-sided craniectomy for evacuation of left-sided hematoma shows a fluid collection in left temporal lobe on T2 (**a**) with some areas of RD on DWI (**b**). These areas are hypointense on ADC (**e**), hyperintense on DWI (**b**) and have some hyperintensity on T1WI (**c**) and hypointense rim on T2WI (**a**) and GRE (**d**) (*arrow*). This represents a hemorrhagic fluid collection and not an abscess as there was no supporting clinical features and patient remained stable for next 9 months. A CT scan (**f**) after 9 months shows interval resolution without any surgery or antibiotic treatment. The DWI has limitations after surgery to detect infection and both sensitivity and specificity are reduced. The presence of T1 hyperintensity due to methemoglobin as seen in **c** and T2 or T2* hypointense rim due to hemosiderin as seen in **a** and **d** are suggestive of hematoma rather than infection

DWI, GRE, and SWI are all very helpful in the evaluation of nonhemorrhagic and hemorrhagic DAI as well as other traumatic injuries on MRI.

Patients with moderate and severe DAI will have obvious findings on the DWI, FLAIR, GRE, and SWI sequences and many patients will even have some abnormalities on the CT to suggest damage to the brain. However, many patients with mild TBI will have a normal or near-normal CT and conventional MRI but will suffer from long-term cognitive problems. Both biomarkers and autopsies have shown that most such patients have microscopic injuries to the white matter tracts which are not revealed by conventional imaging. DTI is a promising tool to diagnose and prognosticate patients with mild TBI and is currently a topic of intense research. However, there is as yet insufficient evidence to support the routine clinical use of advanced neuroimaging studies such as DTI for diagnosis and/ or prognostication of individual patients [66].

17.21 Treatment of Head Injury

Hiroto Kawasaki

Head injury causes damage to the brain through two processes, primary brain injury, and secondary injury. The primary injury occurs at the time
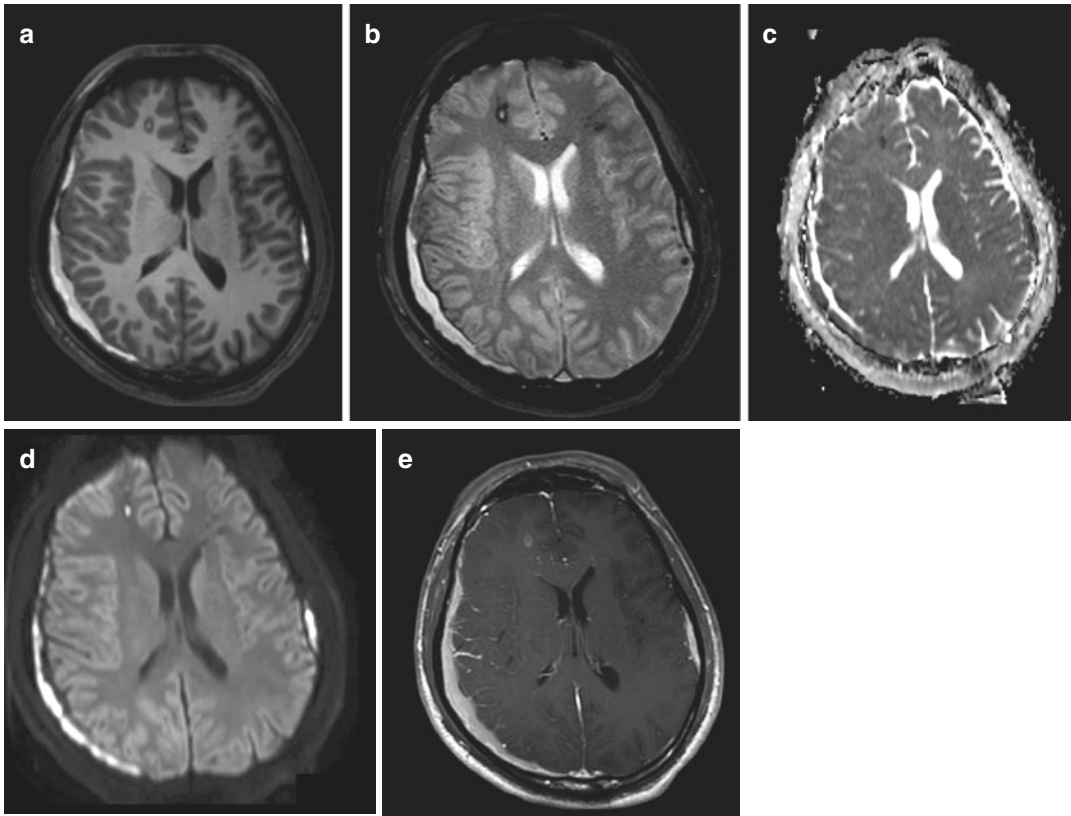
Fig. 17.27 (**a**–**e**) MR brain of 22-year-old male with MVC and ejection shows bilateral subacute SDH which are hyperintense on precontrast T1 (**a**) and show RD on DWI (**d**) and ADC (**c**). There is dural and leptomeningeal enhancement on postcontrast T1 (**e**) on the surface of brain on the right side near the larger SDH due to vascular congestion. RD on DWI and contrast enhancement in a subdural fluid collection may indicate empyema; however history of traumatic SDH and hyperintensity on precontrast T1 and clinical picture should discourage the misdiagnosis

of trauma that include contusion of cerebral cortex or brain stem, and diffuse axonal injury. The secondary injury develops subsequent to the initial injury, such as cerebral edema, intracranial hematoma, ischemia, anoxia, and infection [85]. Head trauma is often associated with other type of injuries in not only head and neck areas but also in other part of bodies which may contribute development of secondary injuries [86]. Treatment of head injury is aimed for controlling the secondary injury because the primary injury is already occurred [87]. The secondary injury develops over wide range of time lines. It is important to predict and find out evolution of the secondary injury in timely manner in order to address promptly to mitigating ongoing problems and preventing further progress of deterioration (Fig. 17.28).

17.21.1 Space-Occupying Lesion

Since the brain is confined in the rigid skull, any increasing volume of pathologic processes increase intracranial pressure, which results in decrease of cerebral perfusion pressure that would subsequently lead to temporary or permanent brain injuries. Such space-occupying lesion includes hematoma in subdural, epidural, and
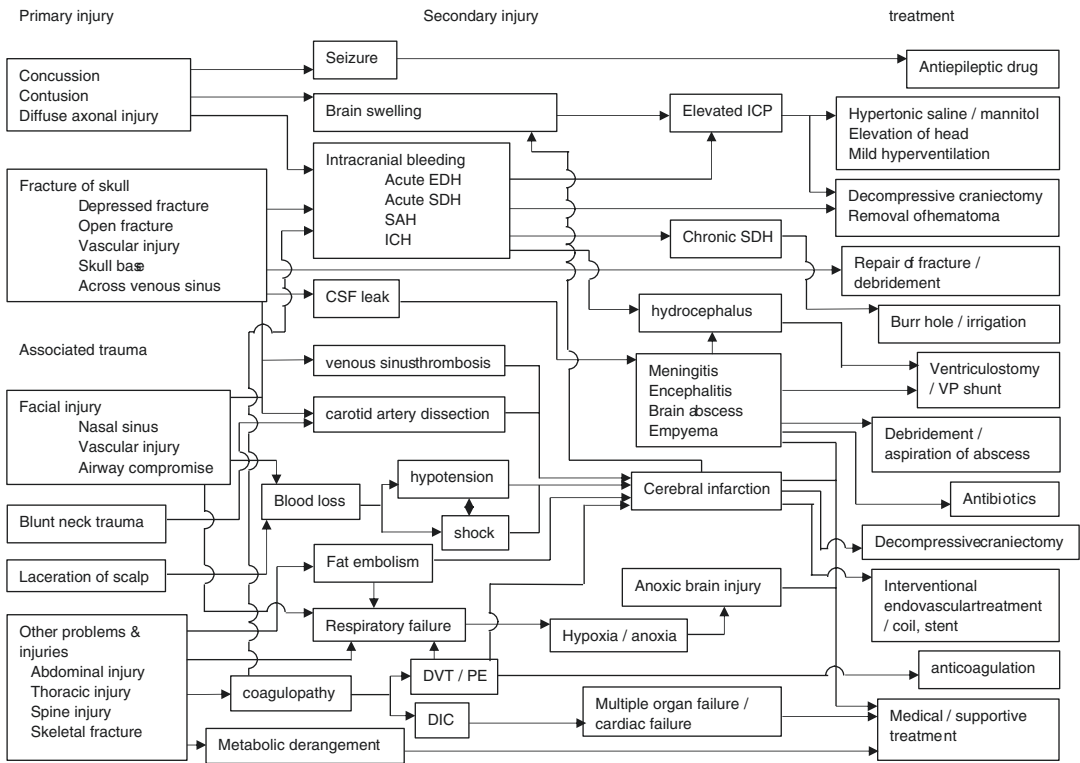
Primary injury   Secondary injury   treatment

Fig. 17.28 Primary/Secondary Injury and Treatment

intracerebral space, hydrocephalus, depressed fracture, foreign bodies, and brain swelling due to contusion, infection, or infarction. Depending on the size, location, and speed of development, some of such lesions must be addressed surgically without delay [86, 88–90]. Goal of surgery is to reduce intracranial pressure. Decompressive craniectomy, removal of space-occupying lesion, and ventriculostomy are often performed.

Open skull fracture and leakage of cerebrospinal fluid render patients to high risk for intracranial infection. Debridement of open wound must be performed in timely manner and if there are free bone fragments they must be removed [91]. CSF leak indicate there are fracture of skull and laceration of dura matter. It may be addressed by placing CSF diversion by either lumbar drain or ventriculostomy. If there is a sizable displaced skull base fracture over the nasal sinus, it often has to be surgically repaired.

Blunt trauma to the head or neck may cause injury to the carotid artery and vertebral artery

[92]. Dissection of major vessel walls may progress into occlusion of the blood vessel in delayed fashion, which could result in cerebral infarction [93]. Dural sinus thrombosis also could occur after head trauma, which may result in elevated ICP and venous infarction of the brain [94].

Patients of head trauma frequently have injuries to other part of body which may affect progression of the secondary brain injury, for example, excessive bleeding either internal or external may cause hypotension and hypoperfusion of the brain [85, 86]. Fractures of long bones or pelvis may cause fat embolism in the brain [95, 96]. Severe trauma regardless of head or body could causes coagulopathy which results in intracranial hemorrhagic disease [97]. Severe trauma also causes derangement of metabolism, for example, hyponatremia is frequently seen after head trauma, which would induce exacerbation of brain swelling and cognitive state [98].

References

1. Gennarelli TA (1993) Mechanisms of brain injury. J Emerg Med 11(Suppl 1):5–11
2. Mutch CA, Talbott JF, Gean A (2016) Imaging evaluation of acute traumatic brain injury. Neurosurg Clin N Am 27(4):409–439
3. Alsop DC, Murai H, Detre JA, McIntosh TK, Smith DH (1996) Detection of acute pathologic changes following experimental traumatic brain injury using diffusion-weighted magnetic resonance imaging. J Neurotrauma 13(9):515–521
4. Gentry LR (1994) Imaging of closed head injury. Radiology 191(1):1–17
5. Kelly AB, Zimmerman RD, Snow RB, Gandy SE, Heier LA, Deck MD (1988) Head trauma: comparison of MR and CT—experience in 100 patients. AJNR Am J Neuroradiol 9(4):699–708
6. Adams JH, Doyle D, Ford I, Gennarelli TA, Graham DI, McLellan DR (1989) Diffuse axonal injury in head injury: definition, diagnosis and grading. Histopathology 15(1):49–59
7. Strich SJ (1956) Diffuse degeneration of the cerebral white matter in severe dementia following head injury. J Neurol Neurosurg Psychiatry 19(3):163–185
8. Gentry LR, Thompson B, Godersky JC (1988) Trauma to the corpus callosum: MR features. AJNR Am J Neuroradiol 9(6):1129–1138
9. Mittl RL, Grossman RI, Hiehle JF, Hurst RW, Kauder DR, Gennarelli TA et al (1994) Prevalence of MR evidence of diffuse axonal injury in patients with mild head injury and normal head CT findings. AJNR Am J Neuroradiol 15(8):1583–1589
10. Abu Hamdeh S, Marklund N, Lannsjö M, Howells T, Raininko R, Wikström J et al (2017) Extended anatomical grading in diffuse axonal injury using MRI: Hemorrhagic lesions in the substantia Nigra and Mesencephalic Tegmentum indicate poor long-term outcome. J Neurotrauma 34(2):341–352
11. Tsitsopoulos PP, Abu Hamdeh S, Marklund N (2017) Current opportunities for clinical monitoring of axonal pathology in Traumatic brain injury. Front Neurol 8:599
12. Gennarelli TA, Graham DI (1998) Neuropathology of the head injuries. Semin Clin Neuropsychiatry 3(3):160–175
13. Hanstock CC, Faden AI, Bendall MR, Vink R (1994) Diffusion-weighted imaging differentiates ischemic tissue from traumatized tissue. Stroke 25(4):843–848
14. Ashikaga R, Araki Y, Ishida O (1997) MRI of head injury using FLAIR. Neuroradiology 39(4):239–242
15. Katayama Y, Becker DP, Tamura T, Tsubokawa T (1990) Cellular swelling during cerebral ischaemia demonstrated by microdialysis in vivo: preliminary data indicating the role of excitatory amino acids. Acta Neurochir Suppl (Wien) 51:183–185
16. Albensi BC, Knoblach SM, Chew BG, O'Reilly MP, Faden AI, Pekar JJ (2000) Diffusion and high resolution MRI of traumatic brain injury in rats: time course and correlation with histology. Exp Neurol 162(1):61–72
17. Assaf Y, Beit-Yannai E, Shohami E, Berman E, Cohen Y (1997) Diffusion- and T2-weighted MRI of closed-head injury in rats: a time course study and correlation with histology. Magn Reson Imaging 15(1):77–85
18. Barzó P, Marmarou A, Fatouros P, Hayasaki K, Corwin F (1997) Contribution of vasogenic and cellular edema to traumatic brain swelling measured by diffusion-weighted imaging. J Neurosurg 87(6):900–907
19. Ito J, Marmarou A, Barzó P, Fatouros P, Corwin F (1996) Characterization of edema by diffusion-weighted imaging in experimental traumatic brain injury. J Neurosurg 84(1):97–103
20. Huisman TAGM, Sorensen AG, Hergan K, Gonzalez RG, Schaefer PW (2003) Diffusion-weighted imaging for the evaluation of diffuse axonal injury in closed head injury. J Comput Assist Tomogr 27(1):5–11
21. Yanagawa Y, Tsushima Y, Tokumaru A, Un-no Y, Sakamoto T, Okada Y et al (2000) A quantitative analysis of head injury using T2*-weighted gradient-echo imaging. J Trauma 49(2):272–277
22. Babikian T, Freier MC, Tong KA, Nickerson JP, Wall CJ, Holshouser BA et al (2005) Susceptibility weighted imaging: neuropsychologic outcome and pediatric head injury. Pediatr Neurol 33(3):184–194
23. Tong KA, Ashwal S, Holshouser BA, Shutter LA, Herigault G, Haacke EM et al (2003) Hemorrhagic shearing lesions in children and adolescents with posttraumatic diffuse axonal injury: improved detection and initial results. Radiology 227(2):332–339
24. Mata-Mbemba D, Mugikura S, Nakagawa A, Murata T, Ishii K, Kushimoto S et al (2018) Traumatic midline subarachnoid hemorrhage on initial computed tomography as a marker of severe diffuse axonal injury. J Neurosurg 129(5):1317–1324
25. Arfanakis K, Haughton VM, Carew JD, Rogers BP, Dempsey RJ, Meyerand ME (2002) Diffusion tensor MR imaging in diffuse axonal injury. AJNR Am J Neuroradiol 23(5):794–802
26. Liu AY, Maldjian JA, Bagley LJ, Sinson GP, Grossman RI (1999) Traumatic brain injury: diffusion-weighted MR imaging findings. AJNR Am J Neuroradiol 20(9):1636–1641
27. Schaefer PW, Huisman TAGM, Sorensen AG, Gonzalez RG, Schwamm LH (2004) Diffusion-weighted MR imaging in closed head injury: high correlation with initial glasgow coma scale score and score on modified Rankin scale at discharge. Radiology 233(1):58–66
28. Takayama H, Kobayashi M, Sugishita M, Mihara B (2000) Diffusion-weighted imaging demonstrates transient cytotoxic edema involving the corpus callosum in a patient with diffuse brain injury. Clin Neurol Neurosurg 102(3):135–139
29. Al Brashdi YH, Albayram MS (2015) Reversible restricted-diffusion lesion representing transient intra-myelinic cytotoxic edema in a patient with traumatic brain injury. Neuroradiol J 28(4):409–412

30. Faden AI, Demediuk P, Panter SS, Vink R (1989) The role of excitatory amino acids and NMDA receptors in traumatic brain injury. Science 244(4906):798–800

31. Moritani T, Smoker WRK, Sato Y, Numaguchi Y, Westesson P-LA (2005) Diffusion-weighted imaging of acute excitotoxic brain injury. AJNR Am J Neuroradiol 26(2):216–228

32. Obrenovitch TP, Urenjak J (1997) Is high extracellular glutamate the key to excitotoxicity in traumatic brain injury? J Neurotrauma 14(10):677–698

33. Borja MJ, Chung S, Lui YW (2018) Diffusion MR imaging in mild traumatic brain injury. Neuroimaging Clin N Am 28(1):117–126

34. Hergan K, Schaefer PW, Sorensen AG, Gonzalez RG, Huisman TAGM (2002) Diffusion-weighted MRI in diffuse axonal injury of the brain. Eur Radiol 12(10):2536–2541

35. Rugg-Gunn FJ, Symms MR, Barker GJ, Greenwood R, Duncan JS (2001) Diffusion imaging shows abnormalities after blunt head trauma when conventional magnetic resonance imaging is normal. J Neurol Neurosurg Psychiatry 70(4):530–533

36. Kin K, Ono Y, Fujimori T, Kuramoto S, Katsumata A, Goda Y et al (2016) The usefulness of CT-diffusion weighted image mismatch in patients with mild to moderate traumatic brain injury. Acta Med Okayama 70(4):237–242

37. Moen KG, Skandsen T, Folvik M, Brezova V, Kvistad KA, Rydland J et al (2012) A longitudinal MRI study of traumatic axonal injury in patients with moderate and severe traumatic brain injury. J Neurol Neurosurg Psychiatry 83(12):1193–1200

38. Bansal M, Sinha VD, Bansal J (2018) Diagnostic and prognostic capability of newer magnetic resonance imaging brain sequences in diffuse axonal injury patient. Asian J Neurosurg 13(2):348–356

39. Kinoshita T, Moritani T, Hiwatashi A, Wang HZ, Shrier DA, Numaguchi Y et al (2005) Conspicuity of diffuse axonal injury lesions on diffusion-weighted MR imaging. Eur J Radiol 56(1):5–11

40. Galloway NR, Tong KA, Ashwal S, Oyoyo U, Obenaus A (2008) Diffusion-weighted imaging improves outcome prediction in pediatric traumatic brain injury. J Neurotrauma 25(10):1153–1162

41. Hou DJ, Tong KA, Ashwal S, Oyoyo U, Joo E, Shutter L et al (2007) Diffusion-weighted magnetic resonance imaging improves outcome prediction in adult traumatic brain injury. J Neurotrauma 24(10):1558–1569

42. Zheng WB, Liu GR, Li LP, Wu RH (2007) Prediction of recovery from a post-traumatic coma state by diffusion-weighted imaging (DWI) in patients with diffuse axonal injury. Neuroradiology 49(3):271–279

43. Biousse V, Suh DY, Newman NJ, Davis PC, Mapstone T, Lambert SR (2002) Diffusion-weighted magnetic resonance imaging in Shaken Baby Syndrome. Am J Ophthalmol 133(2):249–255

44. Epelman M, Daneman A, Halliday W, Whyte H, Blaser SI (2012) Abnormal corpus callosum in neonates after hypoxic-ischemic injury. Pediatr Radiol 42(3):321–330

45. Decaminada N, Thaler M, Holler R, Salsa A, Ladiges C, Rammlmair G (2012) Brain fat embolism. A report of two cases and a brief review of neuroimaging findings. Neuroradiol J 25(2):193–199

46. Rutman AM, Rapp EJ, Hippe DS, Vu B, Mossa-Basha M (2017) T2*-Weighted and diffusion magnetic resonance imaging differentiation of cerebral fat embolism from diffuse axonal injury. J Comput Assist Tomogr 41(6):877–883

47. Stoeger A, Daniaux M, Felber S, Stockhammer G, Aichner F, zur Nedden D (1998) MRI findings in cerebral fat embolism. Eur Radiol 8(9):1590–1593

48. Bodanapally UK, Shanmuganathan K, Shin RK, Dreizin D, Katzman L, Reddy RP et al (2015) Hyperintense optic nerve due to diffusion restriction: diffusion-weighted imaging in traumatic optic neuropathy. Am J Neuroradiol 36(8):1536–1541

49. Budde MD, Skinner NP (2018) Diffusion MRI in acute nervous system injury. J Magn Reson San Diego Calif 1997 292:137–148

50. Irimia A, Wang B, Aylward SR, Prastawa MW, Pace DF, Gerig G et al (2012) Neuroimaging of structural pathology and connectomics in traumatic brain injury: toward personalized outcome prediction. NeuroImage Clin 1(1):1–17

51. Niogi SN, Mukherjee P (2010) Diffusion tensor imaging of mild traumatic brain injury. J Head Trauma Rehabil 25(4):241–255

52. Langlois JA, Rutland-Brown W, Wald MM (2006) The epidemiology and impact of traumatic brain injury: a brief overview. J Head Trauma Rehabil 21(5):375–378

53. Basser PJ, Pierpaoli C (2011) Microstructural and physiological features of tissues elucidated by quantitative-diffusion-tensor MRI. 1996. J Magn Reson San Diego Calif 1997 213(2):560–570

54. Ducreux D, Huynh I, Fillard P, Renoux J, Petit-Lacour MC, Marsot-Dupuch K et al (2005) Brain MR diffusion tensor imaging and fibre tracking to differentiate between two diffuse axonal injuries. Neuroradiology 47(8):604–608

55. Naganawa S, Sato C, Ishihra S, Kumada H, Ishigaki T, Miura S et al (2004) Serial evaluation of diffusion tensor brain fiber tracking in a patient with severe diffuse axonal injury. AJNR Am J Neuroradiol 25(9):1553–1556

56. Inglese M, Makani S, Johnson G, Cohen BA, Silver JA, Gonen O et al (2005) Diffuse axonal injury in mild traumatic brain injury: a diffusion tensor imaging study. J Neurosurg 103(2):298–303

57. Wilde EA, McCauley SR, Barnes A, Wu TC, Chu Z, Hunter JV et al (2012) Serial measurement of memory and diffusion tensor imaging changes within the first week following uncomplicated mild traumatic brain injury. Brain Imaging Behav 6(2):319–328

58. Grossman EJ, Inglese M, Bammer R (2010) Mild traumatic brain injury: is diffusion imaging ready for primetime in forensic medicine? Top Magn Reson Imaging TMRI 21(6):379–386

59. Eierud C, Craddock RC, Fletcher S, Aulakh M, King-Casas B, Kuehl D et al (2014) Neuroimaging after mild traumatic brain injury: review and meta-analysis. NeuroImage Clin. 4:283–294

60. Sidaros A, Engberg AW, Sidaros K, Liptrot MG, Herning M, Petersen P et al (2008) Diffusion tensor imaging during recovery from severe traumatic brain injury and relation to clinical outcome: a longitudinal study. Brain J Neurol 131(Pt 2):559–572

61. Rutgers DR, Fillard P, Paradot G, Tadié M, Lasjaunias P, Ducreux D (2008) Diffusion tensor imaging characteristics of the corpus callosum in mild, moderate, and severe traumatic brain injury. AJNR Am J Neuroradiol 29(9):1730–1735

62. Shenton ME, Hamoda HM, Schneiderman JS, Bouix S, Pasternak O, Rathi Y et al (2012) A review of magnetic resonance imaging and diffusion tensor imaging findings in mild traumatic brain injury. Brain Imaging Behav 6(2):137–192

63. Messé A, Caplain S, Pélégrini-Issac M, Blancho S, Montreuil M, Lévy R et al (2012) Structural integrity and postconcussion syndrome in mild traumatic brain injury patients. Brain Imaging Behav 6(2):283–292

64. Magnoni S, Mac Donald CL, Esparza TJ, Conte V, Sorrell J, Macrì M et al (2015) Quantitative assessments of traumatic axonal injury in human brain: concordance of microdialysis and advanced MRI. Brain J Neurol 138(Pt 8):2263–2277

65. Ljungqvist J, Nilsson D, Ljungberg M, Esbjörnsson E, Eriksson-Ritzén C, Skoglund T (2017) Longitudinal changes in diffusion tensor imaging parameters of the corpus callosum between 6 and 12 months after diffuse axonal injury. Brain Inj 31(3):344–350

66. Wintermark M, Sanelli PC, Anzai Y, Tsiouris AJ, Whitlow CT (2015) American College of Radiology Head Injury Institute. Imaging evidence and recommendations for traumatic brain injury: advanced neuro- and neurovascular imaging techniques. AJNR Am J Neuroradiol 36(2):E1–E11

67. Yuh EL, Cooper SR, Mukherjee P, Yue JK, Lingsma HF, Gordon WA et al (2014) Diffusion tensor imaging for outcome prediction in mild traumatic brain injury: a TRACK-TBI study. J Neurotrauma 31(17):1457–1477

68. Marrale M, Collura G, Brai M, Toschi N, Midiri F, La Tona G et al (2016) Physics, techniques and review of neuroradiological applications of diffusion kurtosis imaging (DKI). Clin Neuroradiol 26(4):391–403

69. Kozak LR, Bango M, Szabo M, Rudas G, Vidnyanszky Z, Nagy Z (2010) Using diffusion MRI for measuring the temperature of cerebrospinal fluid within the lateral ventricles. Acta Paediatr Oslo Nor 1992 99(2):237–243

70. Tazoe J, Yamada K, Sakai K, Akazawa K, Mineura K (2014) Brain core temperature of patients with mild traumatic brain injury as assessed by DWI-thermometry. Neuroradiology 56(10):809–815

71. Miles L, Grossman RI, Johnson G, Babb JS, Diller L, Inglese M (2008) Short-term DTI predictors of cognitive dysfunction in mild traumatic brain injury. Brain Inj 22(2):115–122

72. Kurca E, Sivák S, Kucera P (2006) Impaired cognitive functions in mild traumatic brain injury patients with normal and pathologic magnetic resonance imaging. Neuroradiology 48(9):661–669

73. Kawamata T, Katayama Y, Mori T, Aoyama N, Tsubokawa T (2002) Mechanisms of the mass effect of cerebral contusion: ICP monitoring and diffusion MRI study. Acta Neurochir Suppl 81:281–283

74. Kawamata T, Katayama Y, Aoyama N, Mori T (2000) Heterogeneous mechanisms of early edema formation in cerebral contusion: diffusion MRI and ADC mapping study. Acta Neurochir Suppl 76:9–12

75. Maeda T, Katayama Y, Kawamata T, Yamamoto T (1998) Mechanisms of excitatory amino acid release in contused brain tissue: effects of hypothermia and in situ administration of Co2+ on extracellular levels of glutamate. J Neurotrauma 15(9):655–664

76. Dechambre SD, Duprez T, Grandin CB, Lecouvet FE, Peeters A, Cosnard G (2000) High signal in cerebrospinal fluid mimicking subarachnoid haemorrhage on FLAIR following acute stroke and intravenous contrast medium. Neuroradiology 42(8):608–611

77. Melhem ER, Jara H, Eustace S (1997) Fluid-attenuated inversion recovery MR imaging: identification of protein concentration thresholds for CSF hyperintensity. AJR Am J Roentgenol 169(3):859–862

78. Singer MB, Atlas SW, Drayer BP (1998) Subarachnoid space disease: diagnosis with fluid-attenuated inversion-recovery MR imaging and comparison with gadolinium-enhanced spin-echo MR imaging—blinded reader study. Radiology 208(2):417–422

79. Taoka T, Yuh WT, White ML, Quets JP, Maley JE, Ueda T (2001) Sulcal hyperintensity on fluid-attenuated inversion recovery mr images in patients without apparent cerebrospinal fluid abnormality. AJR Am J Roentgenol 176(2):519–524

80. Wiesmann M, Mayer TE, Yousry I, Medele R, Hamann GF, Brückmann H (2002) Detection of hyperacute subarachnoid hemorrhage of the brain by using magnetic resonance imaging. J Neurosurg 96(4):684–689

81. Kohler R, Vargas MI, Masterson K, Lovblad KO, Pereira VM, Becker M (2011) CT and MR angiography features of traumatic vascular injuries of the neck. AJR Am J Roentgenol 196(6):W800–W809

82. Arbelaez A, Castillo M, Mukherji SK (1999) Diffusion-weighted MR imaging of global cerebral anoxia. AJNR Am J Neuroradiol 20(6):999–1007

83. Berndt M, Lange N, Ryang Y-M, Meyer B, Zimmer C, Hapfelmeier A et al (2018) Value of diffusion-weighted imaging in the diagnosis of postoperative intracranial infections. World Neurosurg 118:e245–e253

84. Farrell CJ, Hoh BL, Pisculli ML, Henson JW, Barker FG, Curry WT (2008) Limitations of diffusion-weighted imaging in the diagnosis of postoperative infections. Neurosurgery 62(3):577–583; discussion 577–583

85. Chesnut RM et al (1993) The role of secondary brain injury in determining outcome from severe head injury. J Trauma 34(2):216–222

86. Bullock MR et al (2006) Surgical management of traumatic parenchymal lesions. Neurosurgery 58(3 Suppl):S25–S46; discussion Si–iv

87. The Brain Trauma Foundation (2000) The American Association of Neurological Surgeons. The Joint Section on Neurotrauma and Critical Care. Initial management. J Neurotrauma 17(6–7):463–469

88. Bullock MR et al (2006) Surgical management of acute subdural hematomas. Neurosurgery 58(3 Suppl):S16–S24; discussion Si–iv

89. Bullock MR et al (2006) Surgical management of acute epidural hematomas. Neurosurgery 58(3 Suppl):S7–S15; discussion Si–iv

90. Bullock MR et al (2006) Surgical management of posterior fossa mass lesions. Neurosurgery 58(3 Suppl):S47–S55; discussion Si–iv

91. Bullock MR et al (2006) Surgical management of depressed cranial fractures. Neurosurgery 58(3 Suppl):S56–S60; discussion Si–iv

92. Stein DM et al (2009) Blunt cerebrovascular injuries: does treatment always matter? J Trauma 66(1):132–143; discussion 143–4

93. Anson J, Crowell RM (1991) Cervicocranial arterial dissection. Neurosurgery 29(1):89–96

94. Ferrera PC, Pauze DR, Chan L (1998) Sagittal sinus thrombosis after closed head injury. Am J Emerg Med 16(4):382–385

95. Riska EB, Myllynen P (1982) Fat embolism in patients with multiple injuries. J Trauma 22(11):891–894

96. Fabian TC et al (1990) Fat embolism syndrome: prospective evaluation in 92 fracture patients. Crit Care Med 18(1):42–46

97. Kaufman HH et al (1984) Clinicopathological correlations of disseminated intravascular coagulation in patients with head injury. Neurosurgery 15(1):34–42

98. Harrigan MR (1996) Cerebral salt wasting syndrome: a review. Neurosurgery 38(1):152–160